T.C.
İSTANBUL UNIVERSITY
INSTITUTE OF GRADUATE STUDIES IN
SCIENCE AND ENGINEERING

M.Sc. THESIS

PLASMON-ENHANCED DYE SENSITIZED SOLAR CELLS

Hüsna AKIN

Department of Chemistry

Chemistry Programme

M. Sc. Student transferred from Fatih University which has been closed

SUPERVISOR
Assoc. Prof. Dr. Ramazan ÖZTÜRK

June, 2016

İSTANBUL

APPROVAL PAGE

This is to certify that I have read this thesis written by Hüsna AKIN and that in my opinion it is fully adequate, in scope and quality, as a thesis for the degree of Master in Chemistry.

Assoc. Prof. Ramazan ÖZTÜRK
Thesis Supervisor

I certify that this thesis satisfies all the requirements as a thesis for the degree of Master in Chemistry.

Yrd. Doç. Dr. Mustafa Demirpolat
vekaleten

Prof. Abdulhadi BAYKAL
Head of Department

Examining Committee Members

Assoc. Prof. Ramazan ÖZTÜRK

Prof. Metin TÜLÜ

Assoc. Prof. Kurtuluş GÖLÇÜK

It is approved that this thesis has been written in compliance with the formatting rules laid down by the Institute of Sciences and Engineering.

Prof. Nurullah ASLAN
Director

June 2016

PLASMON-ENHANCED DYE SENSITIZED SOLAR CELLS

Hüsna AKIN

M.S. Thesis –Science and Engineering
June 2016

Thesis Supervisor: Assoc. Prof. Ramazan ÖZTÜRK

ABSTRACT

A solar is defined as a device that can convert light energy into electric energy on the basis of photo-voltaic effect. Compared to the conventional devices available for energy conversion, a PV device provides greater privileges such as low cost, easy preparation protocols, good performance and environmental compatibility. In regard to the available third generatıon PV devices, dye sensitized solar cell (DSSCs) have attracted greater research attention based on their economic yet efficient approach. Although DSSC have achieved considerable efficiency during a long research period, greater efficiency can be obtained via application of plasmonic nanostructures utilized for improving light absorption, scattering and reflection within the parent DSSC. Plasmonic solar cells are thus, defined as a class of photovoltaic devices that can convert light energy into electricity via applicatıon of plasmonic effect. Cells improve absorption by scattering light using metal nanoparticles excited at their surface plasmon resonance. This allows light to be absorbed more directly without the relatively thick additional layer required in other types of thin-film solar cells. Embedding metal NPs in TiO_2 or ZnO layer typically employed in DSSC devices is a viable option for enhancing the light absorption.

In the conventional construction of DSSCs, the charge recombination takes place dominantly at two possible interfaces: TiO2/dye/electrolyte and transparent-conducting oxide (TCO)/electrolyte.

A substantial and stable increase of the current density Jsc of ruthenium (Ru) based dye sensitized solar cells (DSC) of increase the power conversion efficiency of obtained by plasmonic enhancement.

In this study, we aim to enhance the efficiency of DSCs by combination of Ru based dyes with Ag and/or Au nanoparticles which are plasmonic nanostructures. Decorating TiO_2 photo anode of dye-sensitized solar cell (DSSC) with silver or gold nanoparticles shown to be an effective approach for enhancing device performance via the plasmonic effects.

Keywords: Plasmonic Enhancement, Gold Nanoparticles, Silver Nanoparticles, Dye, Dye Sensitized Solar Cell

PLASMONİK NANOPARÇACIK KATKILI BOYAYA DUYARLI GÜNEŞ PİLLERİ

Hüsna AKIN

Yüksek Lisans Tezi – Fen Bilimleri Enstitüsü
Haziran 2016

Tez Danışmanı: Doç. Dr. Ramazan ÖZTÜRK

ÖZ

Bir güneş pili, fotovoltaik etki temeline dayanarak ışık enerjisini elektrik enerjisine dönüştüren cihaz olarak tanımlanır. Enerji dönüşümü, mevcut konvansiyonel cihazlara kıyaslandığında, bir fotovoltaik cihazı, düşük maliyeti, kolay hazırlanma prosedürü, iyi bir performansa sahip oluşu ve çevre uyumluluğu sayesinde büyük ayrıcalıklara sahiptir. Üçüncü nesil fotovoltaik cihazlar göz önüne alındığında, boyaya duyarlı güneş pilleri (DSSCs) ekonomik oluşu ve veriminden dolayı bir çok araştırmacının ilgisini çekmiştir. Bununla beraber boyaya duyarlı güneş pillerinin araştırma süresi boyunca kayda değer bir verimi olmasına rağmen, plazmonik nano yapıları ve bu yapıların ışık soğurulması, yayılması ve yansıması özellikleri kullanılarak verim daha da arttırılır. Plazmonik güneş pilleri böylece fotovoltaik cihaz olup, plazmonik etkisi sayesinde ışık enerjisini elektrik enerjisin çevirilmesinde kullanılmıştır.Metal nanoparçacıkların sahip oldukları uyarılmış enerjisi ve bunlara ait yüzey plazmon enerjisi saçılan ışık kullanılarak pilin soğurulmasını arttırır. Bu hafif-ince film ışığın daha kalın bir tabaka olmadan doğrudan emilimini sağlar. Tipik boyaya duyarlı güneş pilleri cihazlarında içine TiO_2 veya ZnO tabakasına metal nanoparçacıkların gömülmesi ışık emilimini arttırmak için kullnılan uygun bir seçenektir. Boyaya duyarlı güneş pillerinin konvansiyonel yapısına baktığımızda yüksek ihtimal iki arayüzeyde yük rekombinasyonu mümkündür. Bunlar: TiO2/boya/elektrolit ve şeffaf iletken tabaka (TCO)/elektrolit.

Plasmonik katkılı rutenyum (Ru) bazlı boyaya duyarlı güneş pillerinin sahip olduğu akım yoğunluğunun (Jsc) sabit ve önemli bir artışı, elde edilen güç dönüşüm verimliliğini arttırmıştır.

Bu çalışmada, boyaya duyarlı güneş pillerinin verimini arttırmak için Ru bazlı (N 719) boya ve Gümüş (Ag) ve Altın (Au)'dan oluşan plazmonik nanoyapılar kullanılmıştır. Boyaya duyarlı güneş pillerinde (DSSC) fotoanod olan TiO_2 ile nanoparçacıların dekorasyonu sayesinde plasmonik etki yoluyla cihazın performansının arttırılması beklenmektedir.

Anahtar Kelimeler: Altın nanokafes, Altın nanoküre, Gümüş nanaoküp, DSSC, plazmonik katkılı.

To my parents

ACKNOWLEDGEMENT

I express sincere appreciation to Assoc. Prof. Ramazan ÖZTÜRK. I thank him for his contribution, guidance, patience, experience and support throughout my research.

Thanks go to Dr. Razium Ali SOOMRO, Assoc. Prof. Kurtuluş GÖLÇÜK, Res. Assist Osman GÜRBÜZ, Dr. İsa ŞEKER, Özlem POLAT AKYÜZ for their valuable help, suggestions and comments.

I express my thanks and appreciation to my parents for their understanding, motivation and patience and especially Dr. Razium Ali SOOMRO who encouraged me at my difficult times. Lastly, I extent my gratitude to all colleagues and friends.

TABLE OF CONTENTS

LIST OF TABLE

TABLE

LIST OF FIGURE

FIGURE

LIST OF SYMBOLS AND ABBREVIATIONS

SYMBOL/ABBREVIATION

Au	Gold
Ag	Silver
S	Sulphur
AuNPs	Gold Nanoparticles
AuNS	Gold Nanosphere
AgNC	Silver Nanocube
AuNC	Gold Nanocage
PEG	Polyethylene Glycol
SH-PEG	Thiolated-Polyethylene Glycol
PVP	Poly (vinyl pyrolidone)
PAA	Polyacrylic Acid
DSSC	Dye Sensitized Solar Cell
ITO	Indium Tin Oxide
DI	De-ionized
UV-Vis	Ultraviolent Visible
SEM	Scanning Electron Microscopy
TEM	Transmission Electron Microscopy

CHAPTER 1

INTRODUCTION

1. INTRODUCTION

The proportionally increasing human population with un-quenching demand for energy requires drastic measures for energy fulfillment. Keeping at this pace, the energy requirement is expected to double within the next three decades where energy from fossil fuels and other resources such as nuclear and hydrothermal, wind etc. would not only be insufficient but also un-economic for domestic usage. In contrast energy obtained from solar cell provides much greater economic advantage in terms of abundance and prominent availability. In this regard, isolating solar radiation and transform it into usable form of energy such as electricity or chemical fuel is still a challenging task. In this connection, photo-voltaic devices are the primary system then enable easy and cheap conversion of solar radiation directly into electrical energy. The photo-voltaic devices are more simply called as solar cells[1]. A solar cell or photo-voltaic device by definition is a device that can convert incident photon radiation into electrical energy via production of charge carriers known as electron-hole pair. Although, solar cells have proven vital in production of energy, however there is a need to overcome many challenges to ensure the usage of PV cell in domestic markets. The main challenges to overcome include:

- Higher power conversion efficiency
- Lower production cost
- Increase in product stability

1.2 HISTORICAL EVALUATION OF PV CELLS

The PV technology being utilized today dates back to 1954, when Chapin et al. at Bell[2] demonstrated production of 6% power conversion efficiency (PCE) with silicon solar cell[3].A few years later, their most extensive usage was observed in space exploration.

This was the first generation solar cell fabricated of mono crystalline and poly crystalline silicon solar cell. The increasing technological advance enabled further improvement in first generation solar cell and maximum power conversion efficiency was recovered up to 25 %. Although the PCE values were highly promising, the overall production cost of these solar cell were very high which made them un-suitable candidate from the domestic energy market. The overcome the costliness problem associated with 1^{st} generation solar cell, the 2^{nd} generation solar cell were introduced. The 2^{nd} generation solar cell were composed of gallium arsenide (GaAs, PCE ≈ 28%), cadmium telluride (CdTe, PCE ≈ 20%), copper indium gallium selenide (CIGS, PCE ≈ 20%), etc[4, 5]. The 2^{nd} generation solar cell promoted the PV technology, however the overall production cost of still high to facilitate these cells for domestic usage. The 3^{rd} generation solar cell, which included hybrid solar cell such as DSSC were promising because of their lower production cost and respectable efficiency. Although the associated PCE values were not as good as compared to 1^{st} generation solar cell[6], but these DSSC have very low production cost, environmental impact and very short payback time. Thus, a great deal of research interest has been currently focused to promote the overall efficiency of solar cell. Figure 1.1 shows the trend of PCE % for various types of solar cell with respect to time. As seen, a gradual trend in the increment of PCE % associated with DSSC exist in comparison to other PV competitors[5-7].

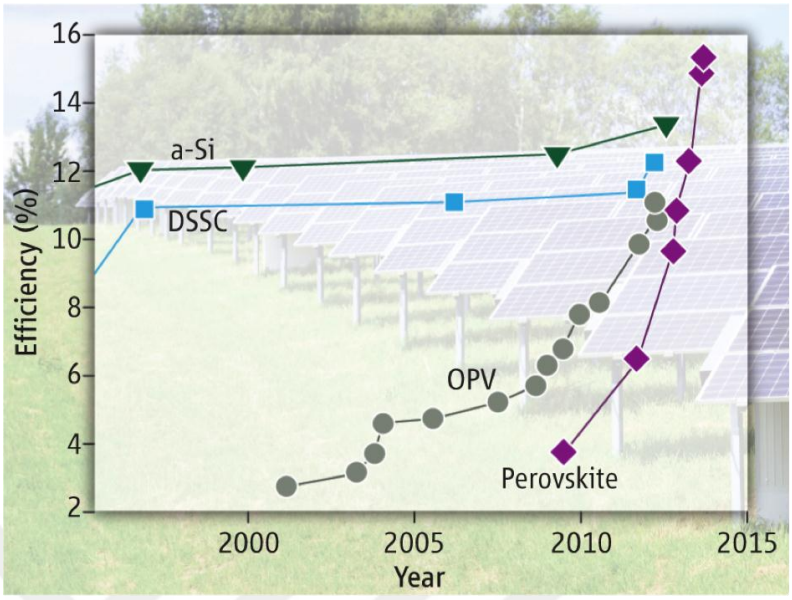

Figure 1.1 Conversion efficiencies of best research solar cells worldwide through 2015 for various photovoltaic technologies.[8]

The improvement in 3rd generation solar cells such as DSSC was most noted from Gratzel[9] and O'Regan[10] group. The constant improvement of DSSC via usage of various electrolytic solution, better interface engineering and plasmonic enhancement have resulted in the promising increment in PCE % from 4 to 12 % with further improvement expected.[11]

1.3 P-N JUNCTION SOLAR CELLS

The PV devices usually employ a P-N junction system for the production of charge carriers. In this assembly, a p-doped and n-doped semiconductor are brought in contact to form a junction. In this condition, the absence of external bias enables electrical field generation at the interface of junction (depletion region).[4, 12] The incident photon absorption from the sun light can create charge carriers such as electrons and holes at this depletion region which are then forced by the built in electrical field to separate. These separated charge carriers are then collected at their respective electrode and as a

consequence become minority carriers allowing more charge separation and current production. The mechanism is illustrated in Figure 1.2.

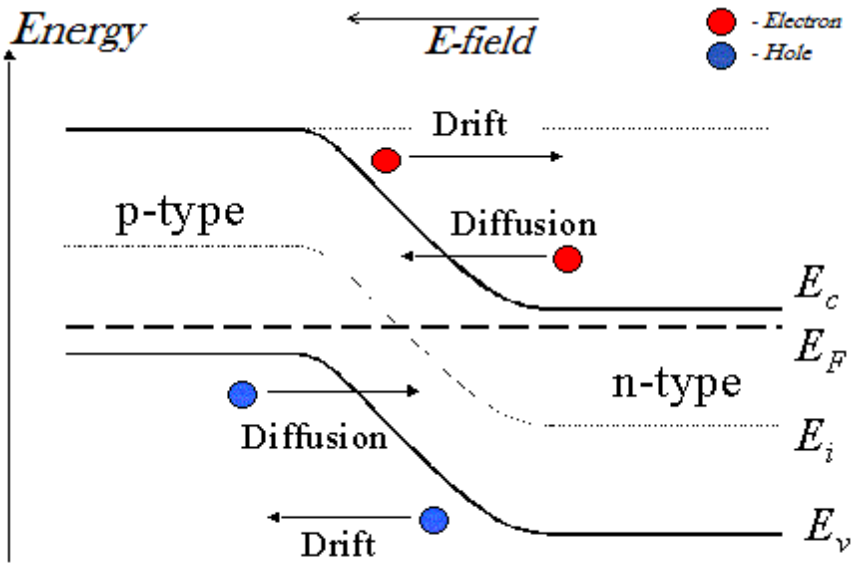

Figure 1.2 A schematic illustration of charge separation in a P-N junction[13]

1.4 SOLAR CELL TERMINOLOGIES

A typical PV solar cell is characterized using number of terminologies associated with its behavior under solar illumination. Most commonly used terminologies include short-circuit current (Isc), open circuit voltage (Voc), fill factor (FF) and efficiency (η).

1.4.1 SHORT-CIRCUIT CURRENT

The short-circuit current is defined as the current noted for solar cell when the total load resistance in equal to zero. It is usually represented as Jsc

$$Jsc = \frac{Isc}{A}\ (mAcm^2) \tag{1.1}$$

Where A is the effective area of the solar cell. Thus, usage of ITO/FTO of 1 cm^2 ×1 cm^2 Jsc would be equal to Isc.

1.4.2 OPEN-CIRCUIT VOLTAGE

The open-circuit voltage is defined as voltage produced from a cell, when infinite load is connected to it. It is mostly connected to the band gap of semi-conductor and charge re-combination within the solar cell. V_{oc} is given as:

$$V_{oc} = \frac{E_{CB}}{q} + \frac{kT}{q} \ln\left(\frac{n}{N_{CB}}\right) - \frac{E_{redox}}{q} \quad \text{(volts)} \tag{1.2}$$

Where n is the number of electrons in the conduction band of TiO_2 and NCB is the effective density of that state.

1.4.3 FILL FACTOR

The fill factor (FF) is the maximum power generated within the solar cell. In simple words, it basically represents the total square area under the I-V curve. It is the ratio of maximum power to the product of Isc and Voc of the fabricated device.

$$FF = \frac{V_m \times I_m}{V_{oc} \times I_{sc}} \tag{1.3}$$

The Vm and Im represents the voltage and current generated at the maximum power point (Pmax). Fill factor can also be associated with the series and shunt resistance of the solar cell. For DSC, it defines the overall extent of electrical losses during its working. It is essential to produce higher FF values which could obtained via improvement in the resistance associated with solar cell.

1.4.4 EFFICIENCY

The efficiency (η) of a solar device is the ratio of Pmax to the energy input from the sun. The mathematical expression is given as follow:

$$\eta = \left(\frac{V_{oc} \times I_{sc} \times FF}{P_{in}}\right) \quad \text{..... (1.4)}$$

The P_{in} is the power input from the sun. However, during measurement of the device, solar radiation is mimicked by using standard conditions given as A.M. 1.5 radiation at 25 °C as shown in the Figure 1.3.[14]

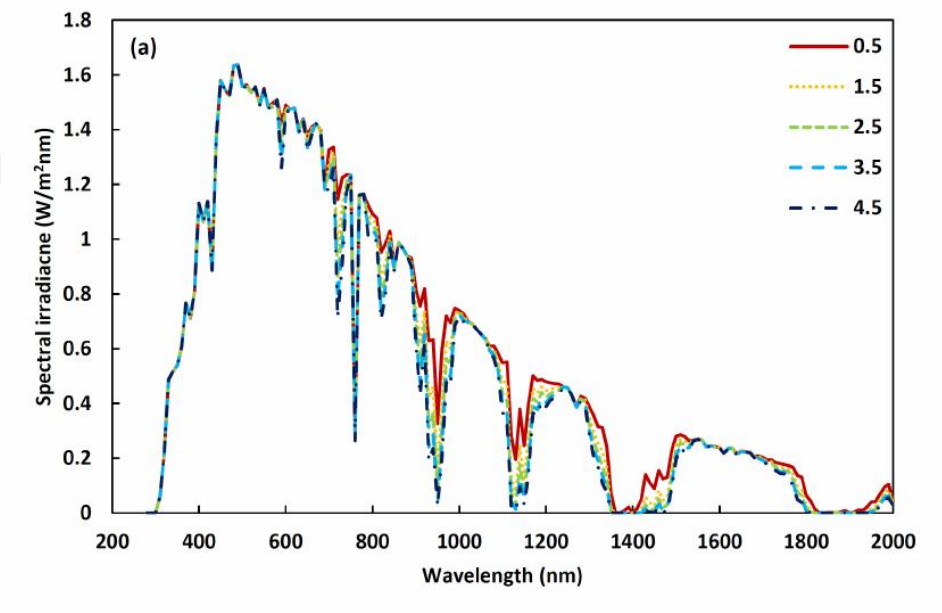

Figure 1.3 The plot of irradiance against wavelength of solar light [15]

1.5 THE CHOICE OF DYE SENSITIZED SOLAR CELL (DSSC)

1.5.1 THE COST EFFECTIVENESS OF THE DSSC

Although, there are numerous PV devices available in the area with relatively large efficiency values however, the DSSC have attracted much greater attention to those, based on its capability to be utilized in domestic power based market. Such capability of DSSC is based on its compatible efficiency values and lower production cost. The cost per watt of DSSC is estimated to be lower than 1$. Despite its low production cost, much efforts are under way to improve the efficiency of DSSC. However, the progress is generally slow due to limitation associated with the utilized sensitizer which is responsible for producing electron[16, 17]. The overall cost per technology can be visualized from the following Figure 1.4.

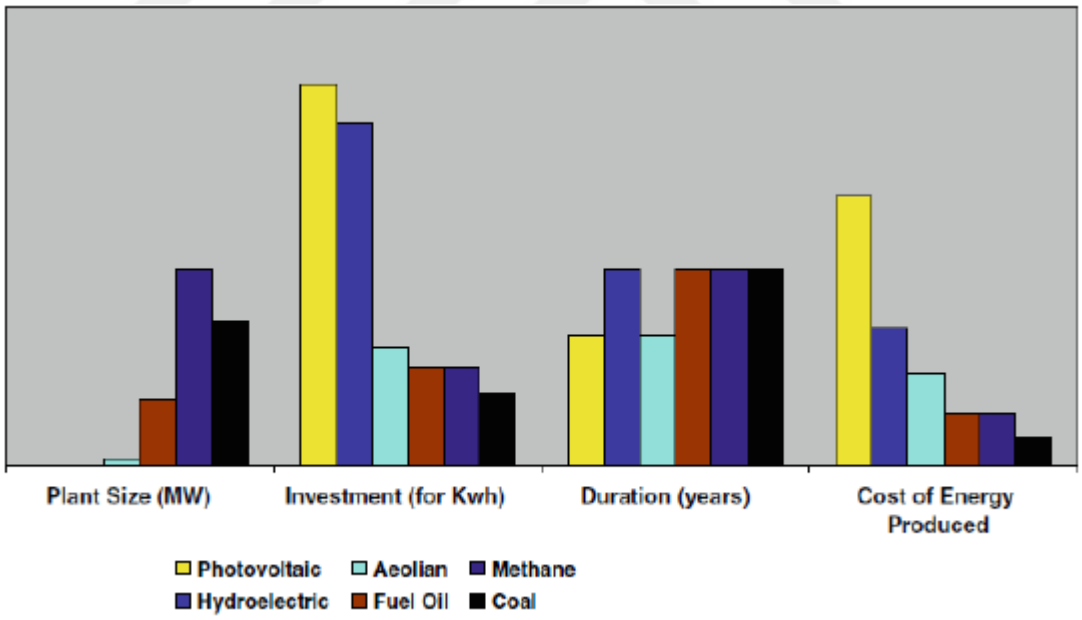

Figure 1.4 The cost of various technology in comparison to photo-voltaic device [13]

1.5.2 THE BASIC OPERATING PRINCIPLE OF DSSC

The DSSC is based on the same working mechanism as that of plants which utilize photo-synthesis to produce electricity from the solar radiation. Figure 1.5 shows a basic configuration of DSSC. The DSSC is based on harvesting light, collecting electron via using separate layer for each process. The operational steps are defined as follow[18]:

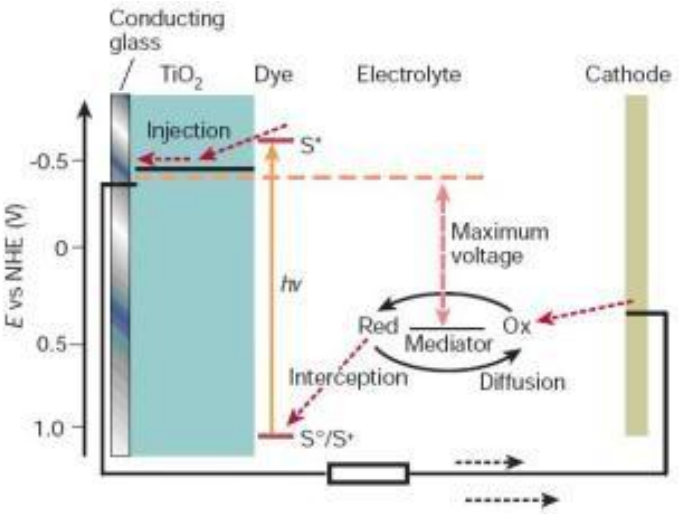

Figure 1.5 Basic device configuration of DSSC [1]

1.5.2.1 THE EXCITATION

The irritation of solar radiation results in absorption of light by sensitizer. The electrons in the sensitizer are excited and transferred to the excited state of the dye. This excitation is relatively short timed and is followed by relaxation to the ground state. The excitation is illustrated in the following equations[19]:

$$S + hU \rightarrow S^*$$

$$S^* \rightarrow S^+ + e^-$$

1.5.2.2 THE INJECTION

The excitation of dye enables dye to transfer electrons to the conduction band of the semi-conductor (TiO_2) due to its close energy levels associated with dye. This charge transfer is

followed by the oxidation of dye. This process is called charge injection and is most efficient when LUMO level of dye has energy higher than of TiO_2[19].

1.5.2.3 THE DIFFUSION WITHIN MESOPOROUS TiO_2

The utilized TiO_2 have oxygen vacancies associated with it which makes its weakly n-doped material. Since, the diameter of used TiO_2 is smaller to produce any electric field, the dominant electron transfer process is mostly diffusion controlled[16, 17].

1.5.2.4 THE IODINE REDUCTION

The dye produced electron travel all the way through ITO and reduces the iodine used as electrolytic solution. In this scenario, the used Pt electrode acts a catalyst for the reduction. The cathodic reaction is given as follow:

$$I_3^- + 2e^- \rightarrow 3I^-$$

The reduction is also fascinated by the excited dye molecules which can result in the recombination of charge carriers. Thus, for improving efficiency of cell, it has to be assured that the ratio of iodine reduction at the counter electrode has to be larger than recombination at TiO_2 electrolytic interface[20, 21].

1.5.2.5 THE REGENERATION OF DYE

The reduced electrolyte replenishes the ground state of the dye (HOMO), enabling its regeneration to original form. Thus, in this way the cycle continuous and electrons are generated for the collection. The replenishment can be illustrated from the following equation[22]:

$$2I^- \rightarrow I_2 + 2e^-$$

1.5 SURFACE PLASMON RESONANCE OF NANOPARTICLES

The Nobel metals such as Ag and Au have the ability to produce a phenomena called as LSPR[23]. When the metallic nanostructures interact with the incoming light, the incident photons are coupled with the conductive band electrons of metal, enabling collective oscillation of the electrons called as localized surface Plasmon resonance. The shape, geometry and size of the particular metal can be manipulated to obtain this LSPR of specific wavelength and energy[24-27]. Plasmonic enhancement is based on this same idea, where LSPR band of a particular metal is engineered as such it overlaps the absorption band of the utilized dye. This enables plasmonic energy transfer to the sensitizer which improves the overall light harvesting capability of the dye.

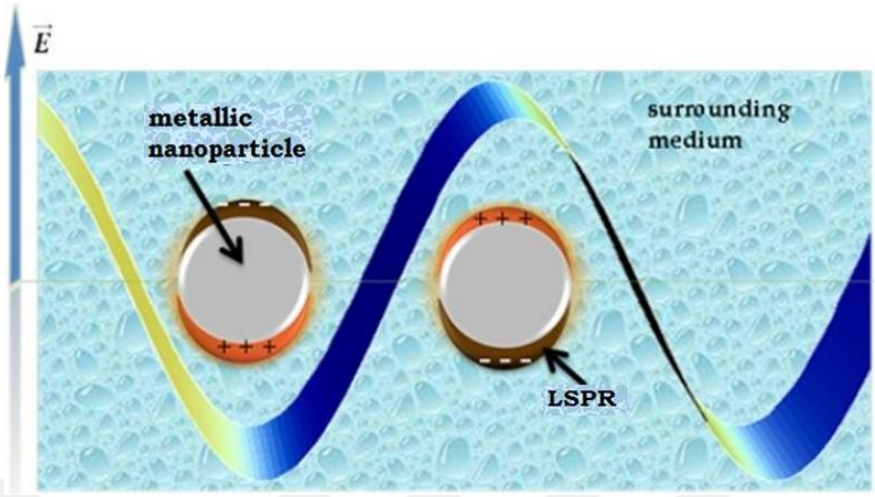

Figure 1.6 Schematic of the electron charge displacement (valence electrons) in a metallic NP (LSPR) interacting with an incident plane wave, with electric field polarized E into a host matrix.[28]

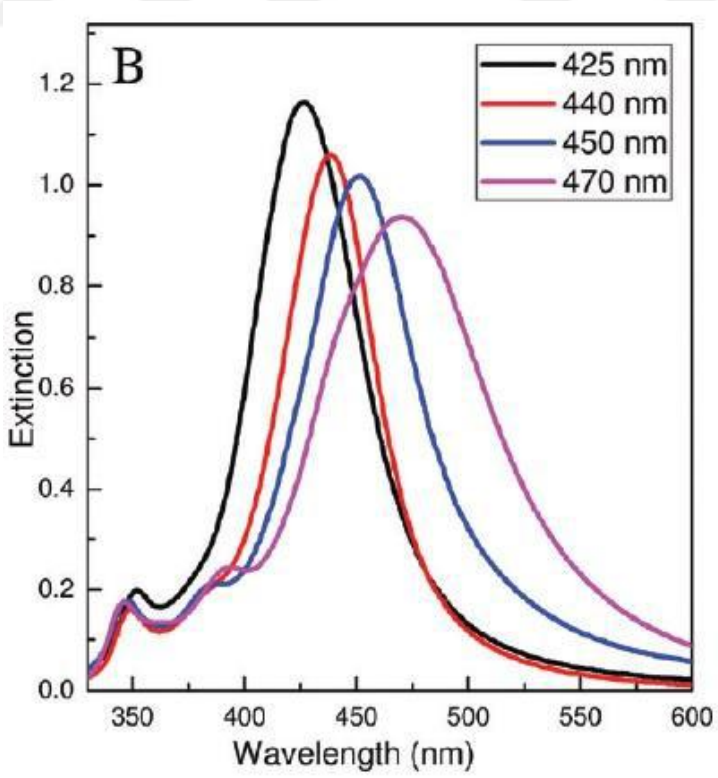

Figure 1.7 SPR of silver nanocubes (AgNCs) with a size of 25, 39, 52, and 86 nm.[29]

1.7 PLASMONIC ENHANCEMENT OF THE DYE SENSITIZED SOLAR CELL

The plasmonic enhancement of a device is associated with many under layered effects such as radiative effect where relaxation of LSPR cause re-radiation into the absorptive layer of the device and works as a secondary light source for enhancement of local electrical field. The second phenomena is called as non-radiative effect, where the relaxation of LSPR enables energy transfer to the vicinal semi-conductor affecting the overall current generation of the device [30, 31]. The utilized metal nanostructures basically act as additional sensitizer in the non-radiative process. The major phenomena's associated with radiative and non-radiative involve incident light scattering, electro-magnetic field and hot electron transfer and plasmonic energy transfer respectively. The major effects are illustrated in the figure 1.8.

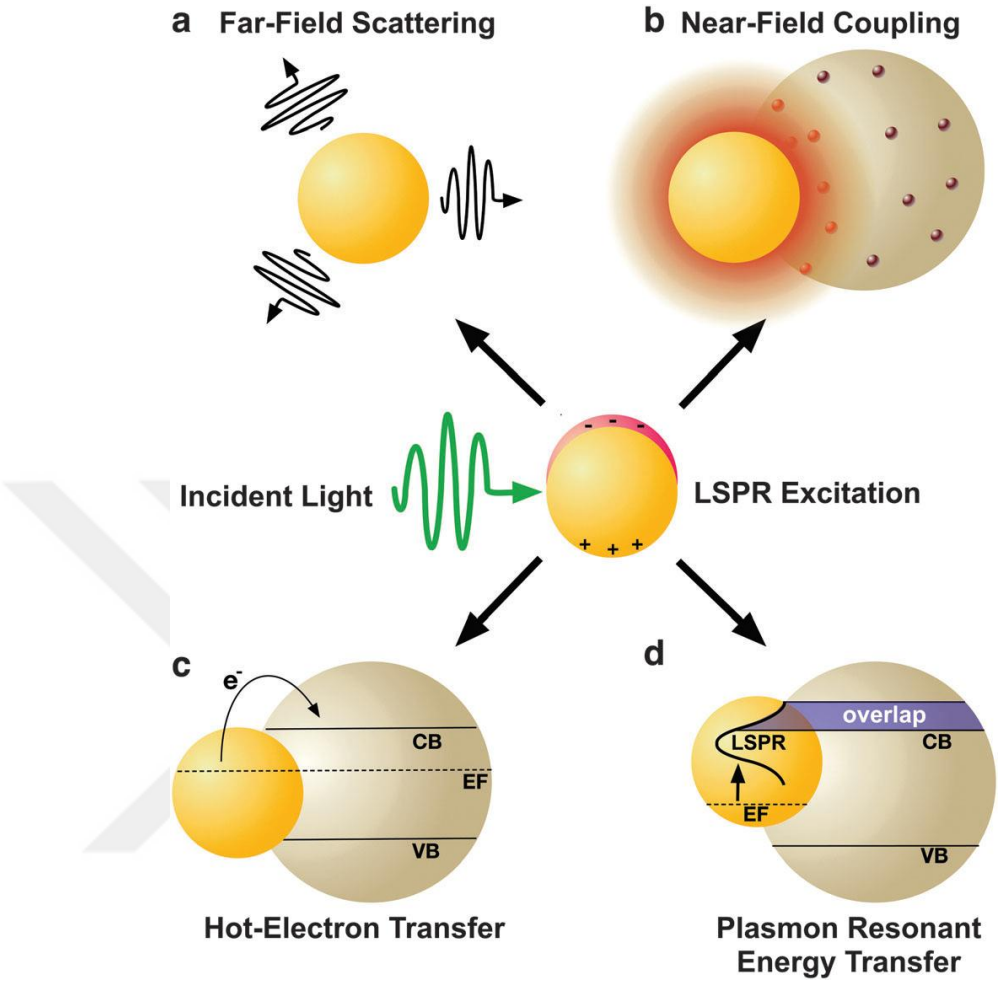

Figure 1.8 Schematic representation of plasmon enhancement processes of radiative effects (a) far-field scattering and (b) near-field coupling; and non-radiative effects: (c) hot-electron transfer, and (d) plasmon resonant energy transfer. [31]

Radiative effect following plasmonic transfer is a finite time process, which can either decay via emitting a photon or by generating an electron-hole pair. This is called as radiative and non-radiative process respectively. The radiative process is responsible for initiating process like near field light scattering. Unlike, near field, the far-field depends on the geometric characteristics of the material. In far-field scattering, the geometrical cross-section of the usually smaller than the scattering cross-section. The scattered light can as a consequence absorb by the distant sensitizer molecules. The multiple scattering that occur via photon encounter with proximal nanostructures increases the overall light trapped

within the mesoporous layer. This particular phenomenon can further be enhanced via tuning the SPR band of the nanostructures within the absorption band region of sensitizer. The near field enhancement is more over a concentrated process occurring near the vicinity of the metal nanostructure itself. It can be understood as the local enhancement of the electro-magnetic radiation which act as secondary source of light increasing the overall photon flux and overall light adsorbed by the mesoporous layer. This near field enhancement is advantages in a sense that, sensitizer molecules residing in the close proximity can easily couple with these electromagnetic radiations and result in enhanced generation of electron-hole pairs.

While, the radiative processes are the most dominant mechanism that govern plasmonic enhancement the non-radiative process like hot –electron transfer (HET) and Plasmon resonant energy transfer (PRET) are the most discussed non-radiative processes. The hot electrons are not in the thermal equilibrium with the atoms in the thermal land and are more specifically known by the effective elevated temperatures. The generation of these electrons is driven by the intra band excitation within the conduction band or via interband excitation from the d-band transitions. Contrary to this, PRET phenomena occurs when resonant energy is transferred from the plasmoinc mental to adjacent semi-conductor via dipole-dipole coupling enabling electron-hole generation at the interface. This PRET can effectively occur only if the selected nanostructures in within the near field range of mesoporous layer. Thus, PRET is highly deepened on the morphology and composition and distance of metal nanostructures from the semi-conducting layer. [31, 32]

1.7.1 SHAPE-DEPENDED PLASMONIC ENHANCEMENT OF DSSC

Although, majority of the reports associated with plasmonic enhanced DSSC primarily focus on the spherical metal nanostructures[32]. A great enhancement has also been achieved using various other morphological shapes such as nanorods, nanocubes, nanoprisms, and core/shell nanostructures [32]. Although, spherical metal nanostructures for gold have proven to overlap with the dye to greater extent, the application of anisotropic structures can provide enhanced light scattering, better spectral tuning and improved

absorption. The panchromatic light absorption capability of such nanostructures can evident contribute towards greater efficiency of DSSC. Figure 1.7 shows the potential plasmonic energy associated with cubic and spherical shape of Au and Ag. As seen, the cubic geometry can heavily contribute towards plasmonic enhancement based on quasistatic light rod effect. This effect allows to build up charge density near the edges of the cube. This concentrated charge density then is responsible for effect plasmonic transfer unlike spheres where charge density is uniformly distributed over the entire spherical surface[31].

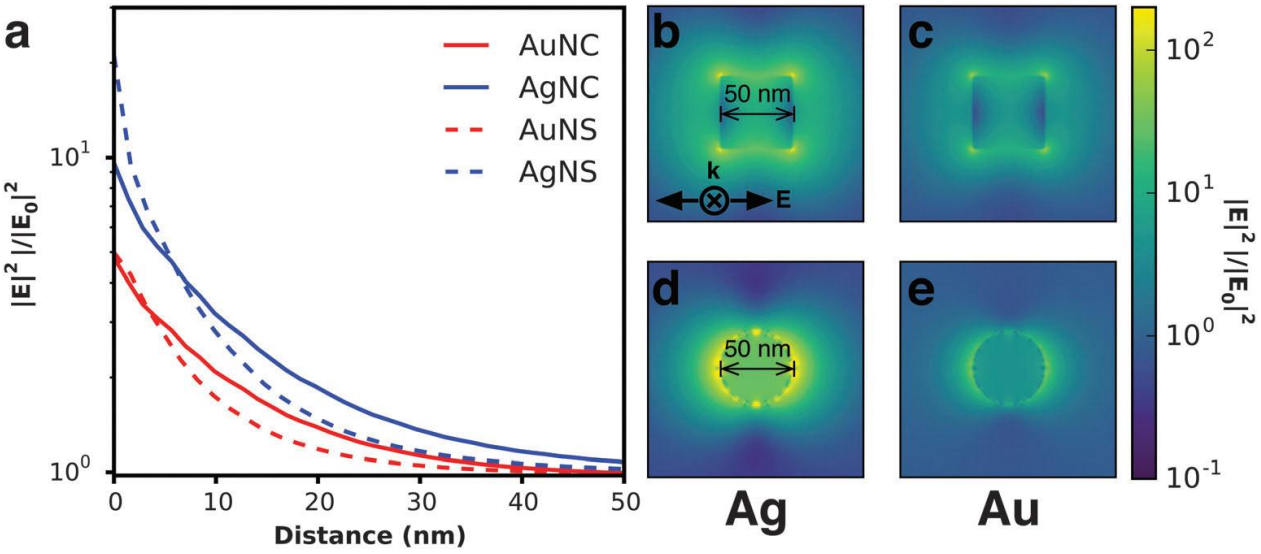

Figure 1.9 (a) The near field enhancement for various plasmonic structures against distance from the particles (b-e) The near field plasmonic profile against geometric shape of Au and Ag of similar size.[31, 32]

In regard to shape dependent plasmonic enhanced DSSC Zarick, H. F., et al. (2014)[32] elaborately studied the variation in total light harvest when size controlled Au nanocubes were integrated with DSSC in comparison to silica coated Au nanocubes. The higher PCE values of Au nanocubes was considered a consequence of intense field localization at the corners of the cube. Such concentration of intense localized field around the edges of the cubes when coupled with the sensitizer not only increases the absorption capability of dye but also results in greater light scattering and production of hot electrons which are then responsible for amplifying the overall efficiency of the system. Although, variety of

different shapes have been explored for their contribution towards light enhancement, however, cavity based structures such as Au nanocages in this context have been less explored. Since, LSPR is large shape dependent with irregular shaped Au nanostructures promoting higher light enhancement in DSSC. This thesis explores the potential capability of cavity based Au nanocages as effective plasmonic subtracts to facilitate larger light trapping in the photo-active layer of DSSC to boost the overall light absorption and power conversion capacity. The experiment details are based on the competitive evaluation of Au nanocages in comparison to Au nanoparticles and Ag nanocube when used in conjunction to N719 dye and I^-/I^-_3 system as effective electrolytic solution.

CHAPTER 2

EXPERIMENTAL PROCEDURE

2.1 MATERIALS

Analytical grade titanium (IV) isopropoxide, titanium (IV) oxide were purchased from Sigma Aldrich, Germany., B2(N719) (ditetrabutylammoniumcis-bis(isothiocyanato)bis(2,2′-bipyridyl-4,4′-dicarboxylato)ruthenium(II)) Dye was obtained from Dyesol., isopropyl alcohol, Acetone, Ethanol, HCI, ITO was obtained TEKNOMA

Hydrogen tetrachloroaurate ($HAuCl_4$), ascorbic acid (formula), silver nitrate ($AgNO_3$), ethylene glycol (formula)(EG), poly(vinyl pyrrolidone) (formula)(PVP, Mn & 55,000), were purchased from Sigma Aldrich, Germany. Sodium sulfide (Na_2S) was obtained from Alfa Aesar, Germany and SAFC, Laysan Bio, Inc. Austria. The stock solution was prepared using de-ionized (DI) water (18.2 MX cm at 25 $^{\circ}$C).

2.2 METHODS

2.2.1 CLEANING THE ITO SUBSTRATES

The ITO substrates ($1\times1cm^2$) used for fabrication of solar cell were prepared using a thorough cleaning process. Initially, the ITO substrates were washed heavily with de-ionized water followed by sonication in boiling de-ionized water for about 5 min. The substrates were then treated with acetone and isopropyl alcohol (IPA) under constant sonication for about 30 min. Finally, the substrates were rinsed with ethanol and dried under stream of nitrogen.

2.2.2 COATING OF THE COMPACT LAYER

The TiO_2 compact layer (C.L) was formed by hydrolysis of $TiCl_4$ aqueous solution. The ITO substrates were immersed in 40 mM $TiCl_4$ aqueous solution at 70 °C for about 15 min to ensure formation of compact scattering layer that would reduce the risk of charge re-combination. The 40 mM $TiCl_4$ solution was prepared by adding titanium tetrachloride to pre-cooled distilled water (~1 °C) in an ice bath[33].

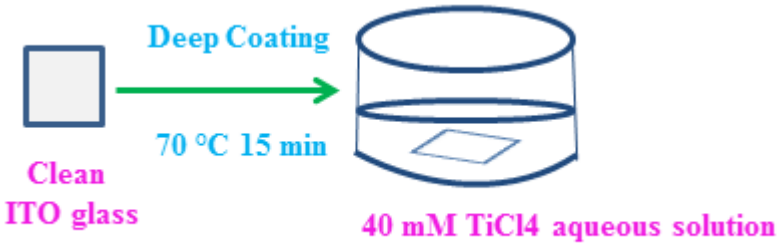

Figure 2.1 TiO_2 compact layer coating of ITO substrate

2.2.3 THE COATING OF MESOPOROUS LAYER

The mesoporous TiO_2 over the pre-cleaned ITO substrates was coated using spin-coating method followed by gradual heat annealiation at 500 °C for about 60 min and ramping at 100 °C in ambient air [34].

The utilized TiO_2 paste was prepared using 0.25 g of powdered TiO_2 mixed with 8 mL of di-ionized and sonicated for about 15 min. The formed slurry was further used for spin coating over ITO glass with spin speed of 2000 rpm with optimum coating volume of 35 µL for about 15 s. This process was repeated five times to achieve a thick yet homogenous TiO_2 layer [35-38].

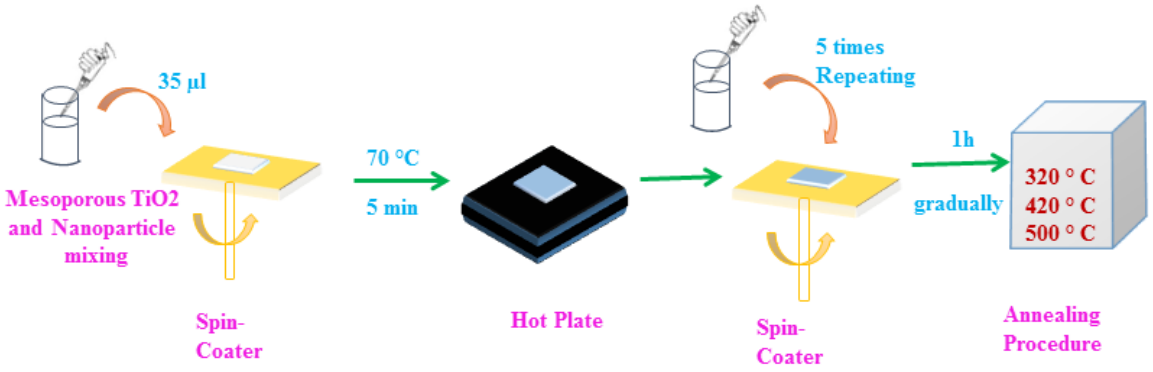

Figure 2.2 Coating the Mesoporous TiO_2 Layer intermixed nanostructure

2.2.4 THE ADSORPTION OF DYE SENSITIZER (N719 DYE)

To introduce the sensitizer layer to the coated mesoporous TiO_2, the pre-coated electrodes were allowed to soak in 0.3 mM N719 dye prepared in anhydrous ethanol for about 24h to achieve complete formation of the photo-anode[22].

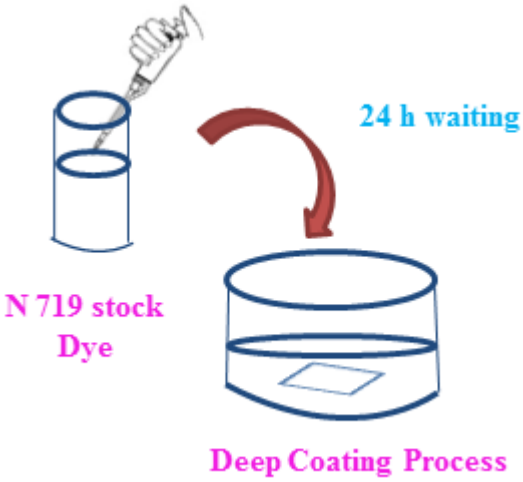

Figure 2.3 Coating of dye sensitize

2.2.5 PREPARING ELECTROLYTE SOLUTION

An I^-/I_3^- redox couple was employed as an active electrolytic solution for the fabricated solar cell. The composition of the electrolyte was 0.5 M KI/0.05 M I_2 (I^-/I_3^-) in solution [21, 39].

2.2.6 SYNTHESIS OF PLASMONIC NANOSTRUCTURES

2.2.6.1 SYNTHESIS OF SILVER NANOCUBE (AgNCS)

The Ag NCs were prepared using previously reported polyol method [23]. In a typical experiment, 35 ml of EG was allowed to heat up to 140 $^{\circ}$C under constant stirring (4000 rpm.) for about 1 hr. The solution was then introduced 10 ml of EG previously containing 0.2 g of PVP (55,000) and set to vortex at 150 $^{\circ}$C for another hr. After complete homogenization, the mixture was introduced 10 ml of EG containing 7.2 mg of Na_2S followed by 5 ml of EG containing 24 mg of Ag NO_3 and vortexed at 100 rpm. until the color of solution shifted from brown to transparent. The solution was kept at rest for about 20 min and again subjected to stirring at 400 rpm until the solution turned non-transparent. The synthesized Ag NCs were extracted from the solvent and extra PVP via high speed centrifugation (13,000) for about 10 min.

2.2.6.2 GOLD NANOSPHERE (AuNS)

AuNSs were synthesized by PVP (MW=10,000) reducing method. Briefly, 20 mL of 1mM $HAuCl_4$ solution was boiled under constant vortex condition for about 10 min. Then 0.1 mM of PVP solution in 10 mL of DI water was added directly inside of the gold solution with continuous stirring. The red color indicated the formation of PVP capped AuNSs.

2.2.6.3 GOLD NANOCAGE (AuNCS)

Au NCs were synthesized according to the study[25]. Briefly, 20 mL of previously prepared silver nanocube template (~40 nm) was first cleaned and heated up to boiling with stirring rate of 300 rpm. $HAuCl_4$ solution (0.1g/ L) was injected slowly until the SPR spectrum peak of the solution shifted to 600 nm. The AuNCs solutions were then continuously refluxed until their absorption spectrum became stable and the solution was then cooled down to room temperature. The solution was kept at room temperature overnight and AgCl was filtered off from the solution.

2.3 ADDITION OF PLASMONIC NANOSTRUCTURES IN DSSC

The plasmonic nanostructures integrated within DSSC were optimized for two different configurations i.e. intermixed within and onto the mesoporous TiO_2[40]. The experimental evidences suggested optimum performance with configuration involving mixing of plasmonic nanostructures within mesoporous layer.

2.4 FABRICATION OF DYE SENSITIZED SOLAR CELL

The Plasmonic DSSC was fabricated using sandwich method. In a typical assemble pre-cleaned ITO glasses (1cm ×1 cm) were treated with 40 mmol·L^{-1} $TiCl_4$ aqueous solution at 70°C for 15 min to obtain a compact layer. The mesoporous absorbing layer (TiO_2) was spin coating 35 µL of titania paste containing 0.35 g TiO_2 (20 nm), 0.5µL and 0.03 mM of Plasmonic nanostructures. The procedure was repeated five time to obtain a thick yet uniform mesoporous layer. The ITO glasses were the annealed at 450 °C followed by immersion in N719 dye (0.03 M in ethanol) for about 24 h to achieve complete formation of the photo-anode. The platinium (Pt) coated ITO glass was utilized as counter electrode for the configured solar cells with 0.5 M KI/0.05 M I_2 (I^- /I_3^-) as electrolytic solution. The finally obtained cells were known to have configuration of compact layer/ TiO_2-plasmonic nanostructures/Dye/Pt-counter electrode.

CHAPTER 3

RESULT&DISCUSSION

3.1 CHARACTERIZATION OF PLASMONIC NANOSTRUCTURES

3.1.1 OPTICAL CHARACTERIZATION

The optical evaluation was carried using UV-Vis spectrophotometer in range of 300 to 800 nm. The absorption spectra for Ag NCs, Au NSs and Au NCs were recorded and evaluated in comparison to absorption spectrum of N719 as shown in Figure 3.1 The maximum absorption noted for Ag NCs, Au NSs and Au NCs was noted around 420, 520 and 600 nm respectively. The observed excitations were found in good agreement with those reported in literature.[27, 41, 42]Unlike, Au NCs and Ag NCs the Au NSs were noted to have maximum overlap with absorption spectra of N719 dye (Figure 3.1). This clearly indicates the capability of Au NSs to participate within the plasmonic enhancement of the DSSC under study. The cavity based structures such as nanocages, nanoboxes and porous particles have the tendency to demonstrate phenomena commonly known as **cage confinement effect** (Figure 3.2). Although such phenomena have been heavily studied for catalytic reaction based on metal nanostructures, however similar scenario can also be presumed for plasmonic enhancement of absorption capability of N719 dye with the application of Au NCs. To experimentally test, the suggested hypothesis UV-Vis spectra were recorded for the fixed concentration of Au NCs and Au NSs against time with gradual addition of N719 dye (0.01 mM). The corresponding graphs are shown in Figure 3.2 (a) The very small decrease in the absorbance band associated with Au NSs with the selected time line clearly depicts the surface bound interaction of dye molecules with Au NSs. Contrary to this, Au NCs Figure 3.2 (b) demonstrate significant decrease in absorption

within initial time range with formation of plateau at higher time reflecting the saturation of the Au nanocages cavity after certain period of dye adsorption.

It has been previously observed that cage containing structures demonstrates a phenome commonly known as **cage confinement effect**. This effect is well studied in catalyst and electrochemical process.[24, 43] However, we were also interested to observe the effect of cavity on the in-coming dye molecules and hence forth we designed this little experiment using UV spectrophotometer.

Since, based on cavity, we believe that the dye molecules would interact with wall of the cage and then with time diffuse within the cavity. This would allow a highly feasible metal-ligand interaction based on the higher surface area offered by the cavity of the cage, and thus, enabling faster and greater electron transfer from metal to dye molecules which would result in decrease of SPR. This situation is clearly evident when a fixed concentration of Au NCs were introduced with small volume of dye solution. As seen in Fig 3.2 on right hand side. The constant decrease in the SPR band of Au NCs is evident of this cage confinement of dye molecules within cavity. In contrast, Au NSs shows different behavior as the SPR band under similar condition only slightly changes which indicates the interaction is surface-bound. More study is underway to explore this phenomenon.

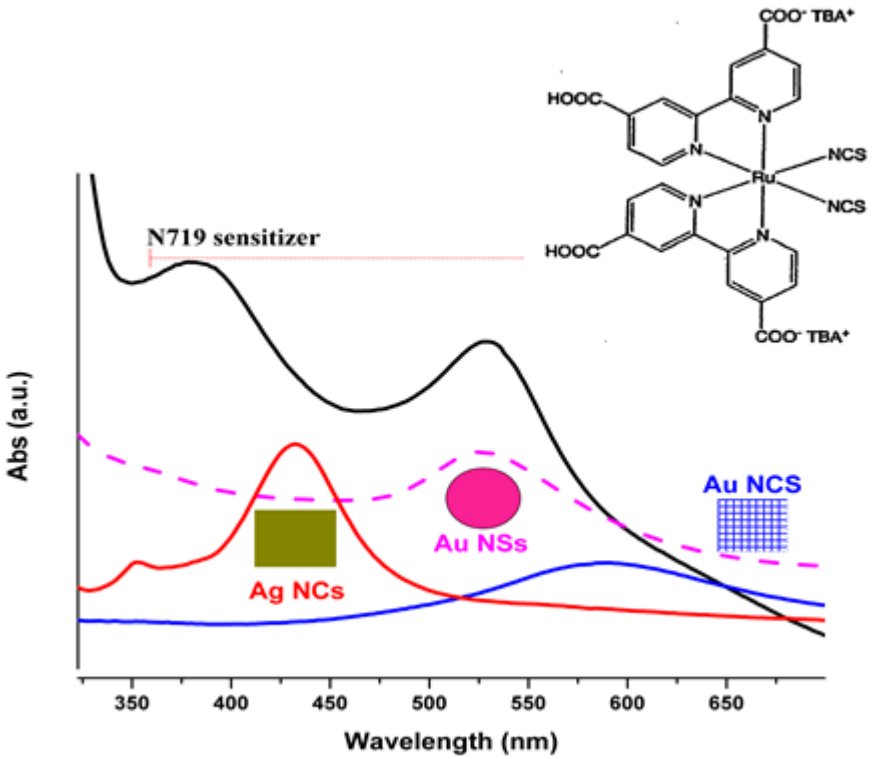

Figure 3.1 UV-visible absorption spectrum of N719 dye overlapped with LSPR spectra of Ag NCs, Au NSs and Au NCs

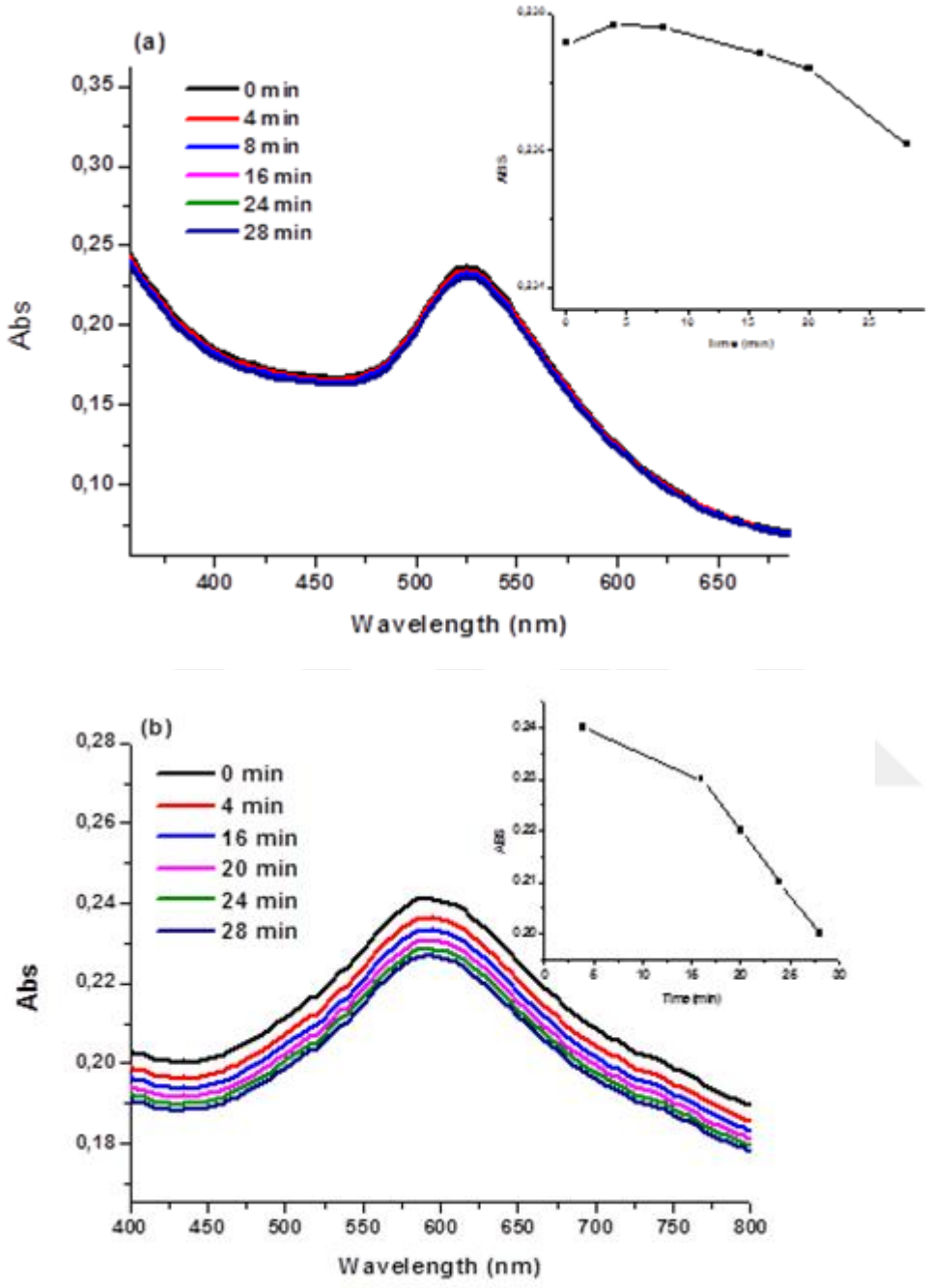

Figure 3.2 UV-Vis spectra recorded for the fixed concentration of (a) Au NSs and (b) Au NCs against time with gradual addition of N719 dye (0.01 mM).

3.1.2 FTDT ANALYSIS OF AS-SYNTHESIZED NANOSTRCTURES

As observed from the FDTD diagrams obtained for Ag NCs, Au NSs and Au NCS the energy associated with these nanostructures is widely dispersed both at the corners and centers of the nanostructures. However, clear distinction can be seen the energy distribution within all the structures. Ag nanocubes based on their solid core and surface displays energy centers at the corners of the cube. Such energy center as the consequences of what is known as quasi-light rod effect [44-47] . Such phenomena occur as a consequence of subcritical flow of energetic photos due at the corners of the cube. This energy as seen in Figure 3.3(a) is then concentrated at the corners of the cube where by it can be easily adsorbed by the sensitizer molecules standing nearby. Contrary to Ag NCs, Au NSs shows quit different scenario. As seen in the Figure 3.3 (b) the energy distribution is moreover limited to rounded edges of the sphere. This in contrast to Ag NCs is more likely not to be efficient in transfer process, as most of the energy is diffused and not concentrated enough to be to transferred to far-standing sensitizer molecules. Besides this it is known that cubic shaped surfaces have more effective surface area compared to spherical shapes. Thus, much lower number of sensitizer molecules can be associated with the spherical corners compared to flat surface offered by cube. Interestingly, the Au NCS displays energetic centers both at corners and within the cavity associated with it. Such distribution of energy is relatively more efficient compared to its other competitors based on the greater surface area offered for adsorption of sensitizer molecules. The Au nanocages with both its internal and external surface area offers much larger platform for plasmonic transfer compared to Ag NCs and Au NSs. Besides this the cavity allows large number of sensitizer molecules can easily diffuse within where maximum plasmonic energy can easily transferred due to excellent interaction of sensitizer with the internal walls of the cage.

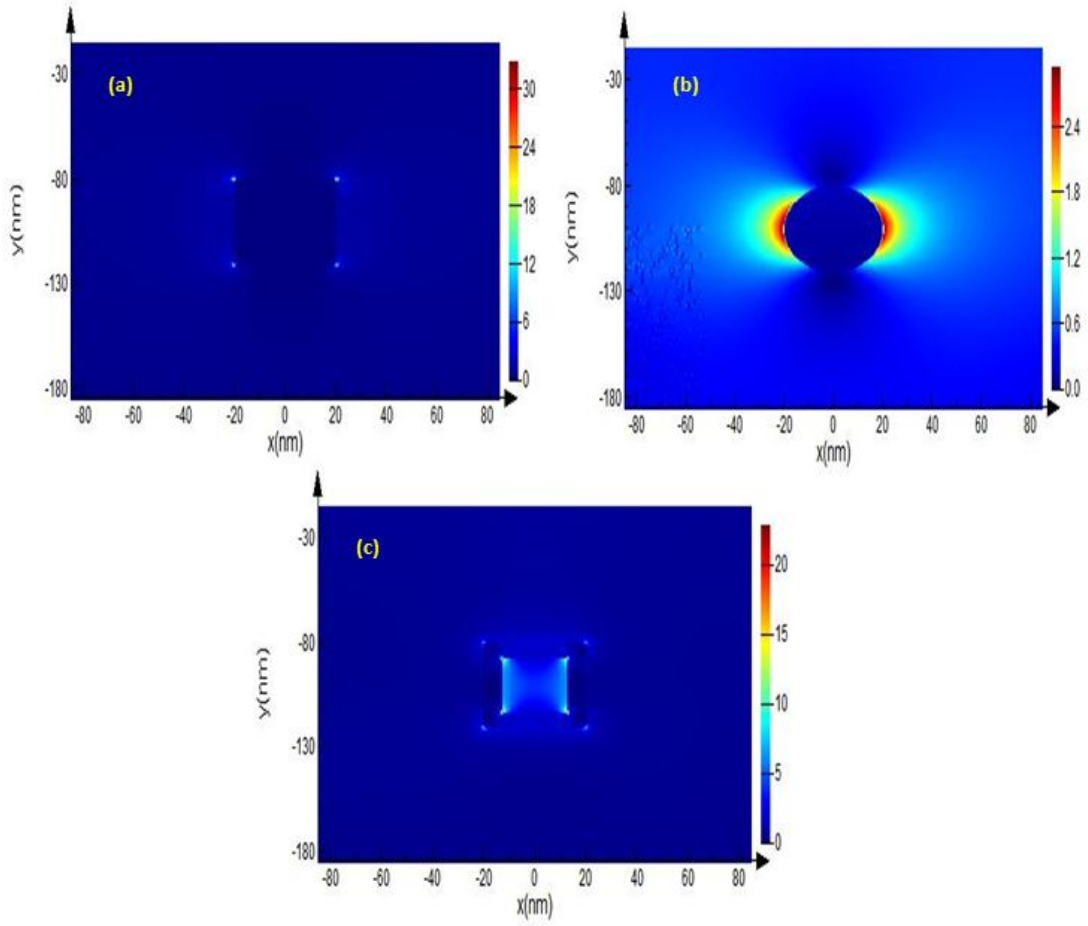

Figure 3.3 FDTD analysis of (a) Ag nanocube (b) Au nanosphere and (c) Au nanocages displaying energy distribution.

3.2 MORPHOLOGICAL CHARACTERIZATION OF THE SYNTHESIZED PLASMONIC NANOSTRUCTURES

The structural evaluation of the synthesized noble metal nanostructures was carried using SEM and TEM. Figure 3.4 (a-c) shows the SEM images of Ag NCs, Au NSs and Au NCs. As seen, the synthesized nanostructures possessed distinct structural features with well dispersed nature and distribution. The average size of Ag NCs were determined to be in range of 45 nm, whereas Au NSs and Au NCs were examined to be in range of 15 and 45 nm. Further evaluations of the morphological characteristics were obtained using TEM analysis. The TEM images shown in figure 3.5 reflects the excellent surface morphology associated with the plasmonic nanostructures. The average size of the plasmonic

nanostructures estimated from the TEM equal to 20, 40 and 60 nm for Ag NCs, Au NSs and Au NCs respectively.

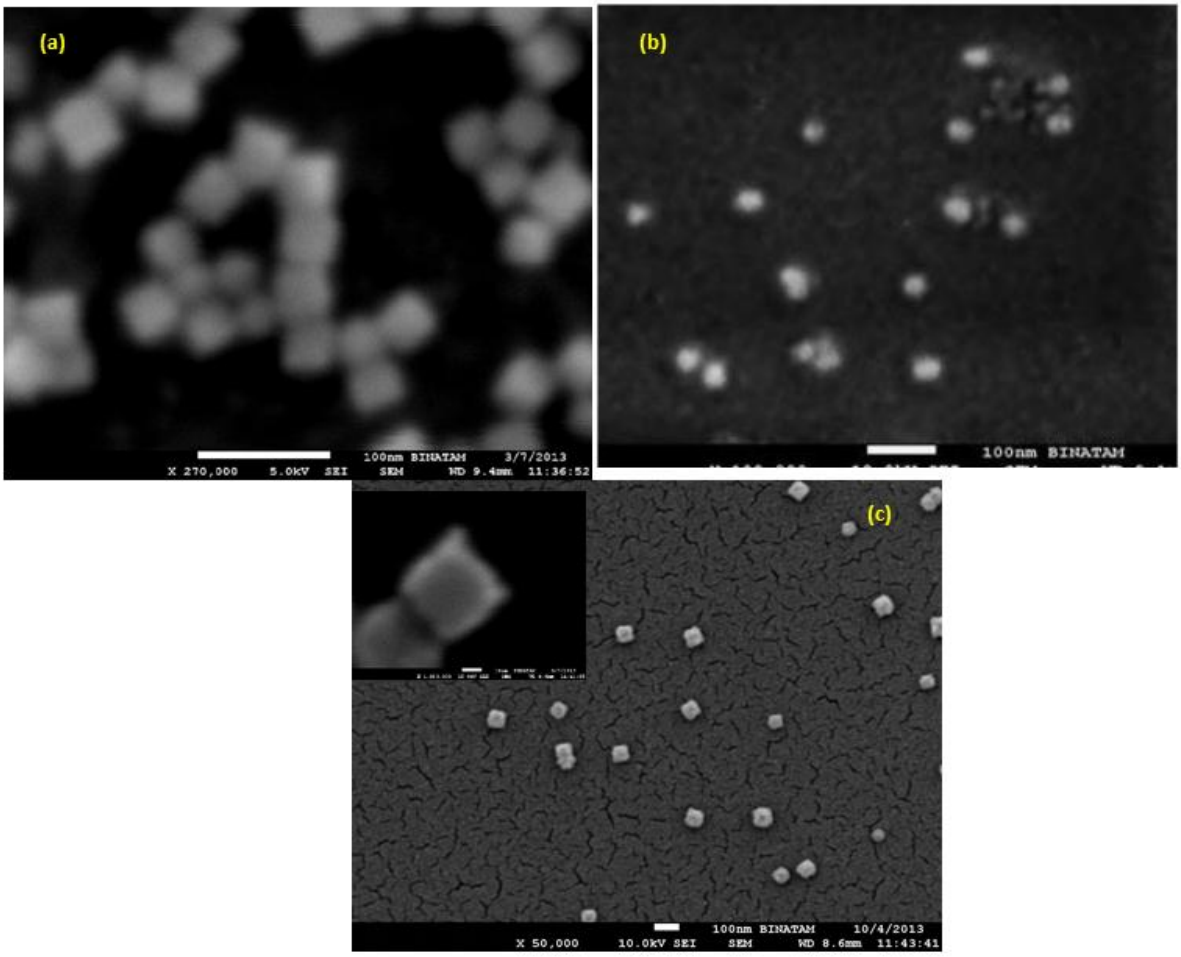

Figure 3.4 SEM images of (a) Ag NCs (b) Au NSs and (b) Au NCs

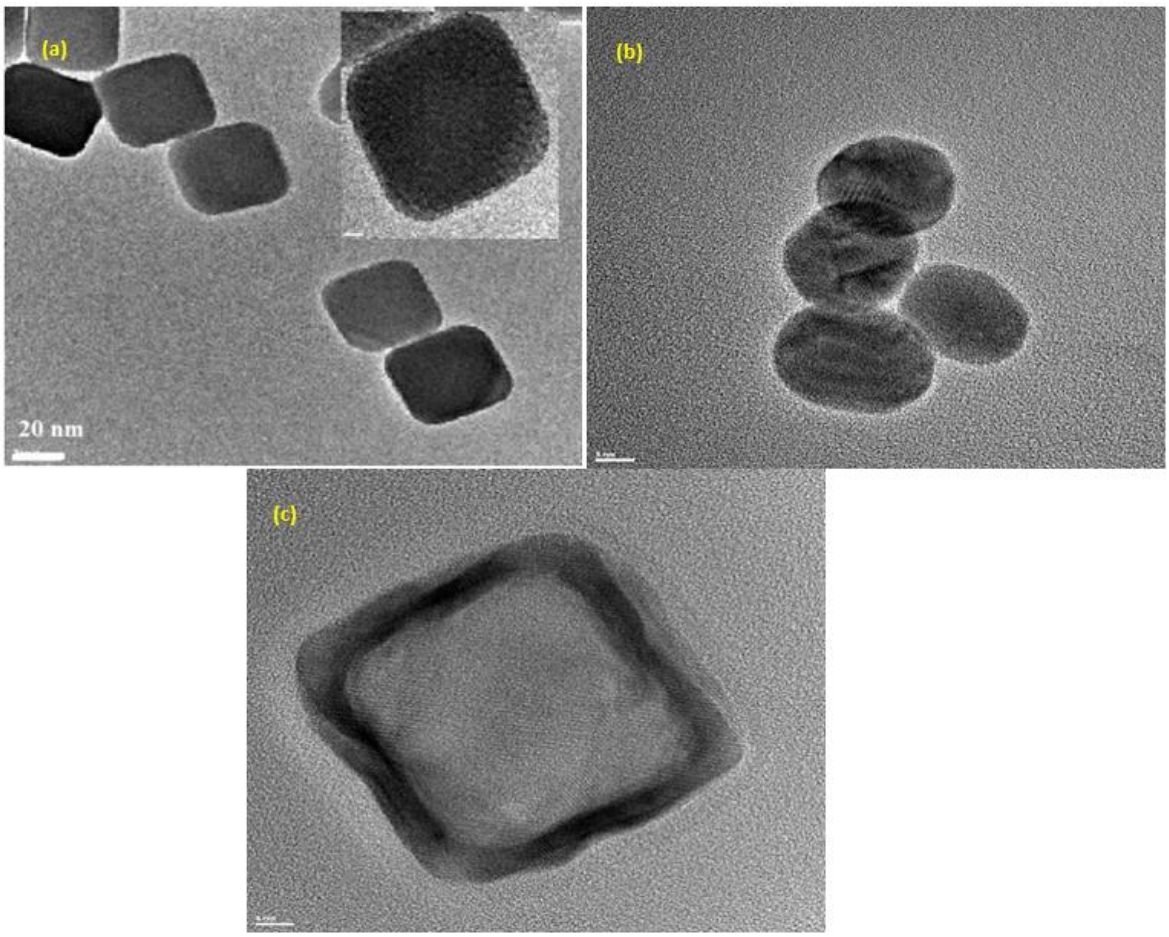

Figure 3.5 TEM images of (a) Ag NCs (b) Au NSs and (c) Au NCs

3.3 MORPHOLOGICAL CHARACTERIZATION OF PLASMONIC NANOSTRUCTURES INTEGRATED MESOPOROUS ANODIC LAYER

The ensure proper intermixing of synthesized plasmonic nanostructures within the mesoporous Titania, SEM and EDX mapping analysis was carried for all the devised configurations of anodic layer. Figure 3.5 (a) shows the SEM image of bare titania layer coated over pre-cleaned ITO glass with inset figures representing the corresponding EDX mapping. The thickness of the coated layer was estimated from the cross-sectional analysis of the coated layer (inset Figure 3.5)

As seen, the coated TiO_2 has homogenously covered the entire area with good uniformity in particle and distribution. The estimated size of TiO_2 from SEM analysis is

determined to be about 20 nm. The SEM image form TiO_2 mixed Ag NCs (TiO_2/Ag NCs) is shown in Figure 3.6 (b). The presence of Ag NCs within the titania is clearly evident whereas, the homogenous distribution of said nanostructures is further reflected from the corresponding EDX mapping. Although the size of titania and Ag NCs is different, however the application of spin coating for the mixed system enabled excellent coverage of ITO glass which as a consequence had greatly influenced the generation of photo-current in the devised photo-anode. Similarly, the SEM images for TiO_2/Au NSs and TiO_2/Au NCs is shown in Figure 3.6 (c-d). The images not only depict the presence of plasmonic nanostructures retaining their distinct morphology but also reflects the homogeneity in their distribution evident from the corresponding EDX color mapping.

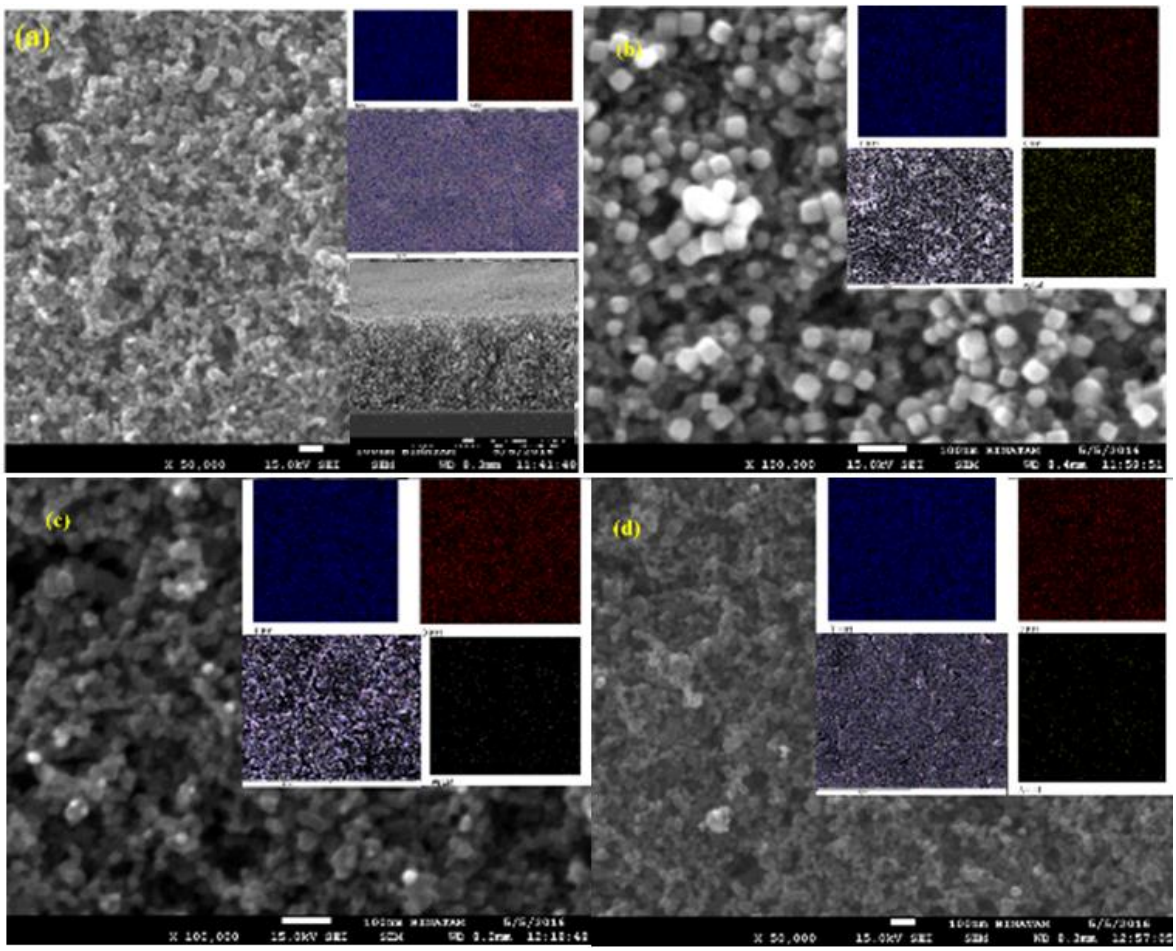

Figure 3.6 Shows the FE-SEM image with corresponding EDX mapping analysis of (a) TiO_2 (b) TiO_2/Ag NCs (c) TiO_2/Au NSs and (d) TiO_2/Au NCs.

3.4 EVALUATION OF VARIOUS CONFIGURATIONS DEVISED FOR PLASMONIC DYE SENSITIZED SOLAR CELL

The Plasmonic nanostructures based DSSC were fabricated using simple layer to layer coating method with Plasmonic nanostructures sandwiched both inside the mesoporous layer and onto the mesoporous layer. From the literature perceptive, various assemble configuration have been adopted to promoted the charge Plasmonic charge transfer from Plasmonic nanostructures to the sensitizer. As suggested in case of Au NSs, the coupling of incident radiation with saturated electron density of plasmonic metal results in photon energy distribution to greater population of electrons. This scenario would not allow the generated electrons to overcome the Schottky barrier (1.0V) associated at the metal-TiO2

interface.[40] However, it has been observed that an ultrafast (<240fs) transition enables Plasmonic assisted electron transfer from metal to TiO_2 particles. The mechanism is schematically represented in Figure 3.7 for better understanding. As observed, the bending associated with mixing of Plasmonic nanostructures within mesoporous titania enables easy transfer of photo electrons from metallic nanoparticles to TiO_2. Henceforth, usage of Plasmonic nanostructures mixed within mesoporous layer can enable transfer of photo-excited electrons of dye to be transferred to conduction band of TiO_2. This in addition to the transfer of hot electrons can simultaneously enhance the total light harvest and photo-current production of DSSC. Herein, the devised solar cells were fabricated using both assemble configuration (into & onto mesoporous TiO_2) where experimental evidences suggested optimum performance with configuration involving mixing of Plasmonic nanostructures within mesoporous layer.

The assembled cell used for measurıng I-V characteristics can be described with following configuration:

1. **Plasmonic nanostructures free DSSC**

(a) C.L/ TiO_2/ N7/ Pt

2. **Plasmonic nanostructures sandwiched onto the mesoporous layer**

(a) C.L/ $TiO_2(Au\ NSs)_{onto}$/ N7/ Pt

3. **Plasmonic nanostructures sandwiched into the mesoporous layer**

(a) C.L/ $TiO_2(Ag\ NCs)_{into}$/ N7/ Pt

(b) C.L/ $TiO_2(Au\ NSs)_{into}$ / N7/ Pt

(c) C.L/ $TiO_2(Au\ NCS)_{into}$ / N7/ Pt

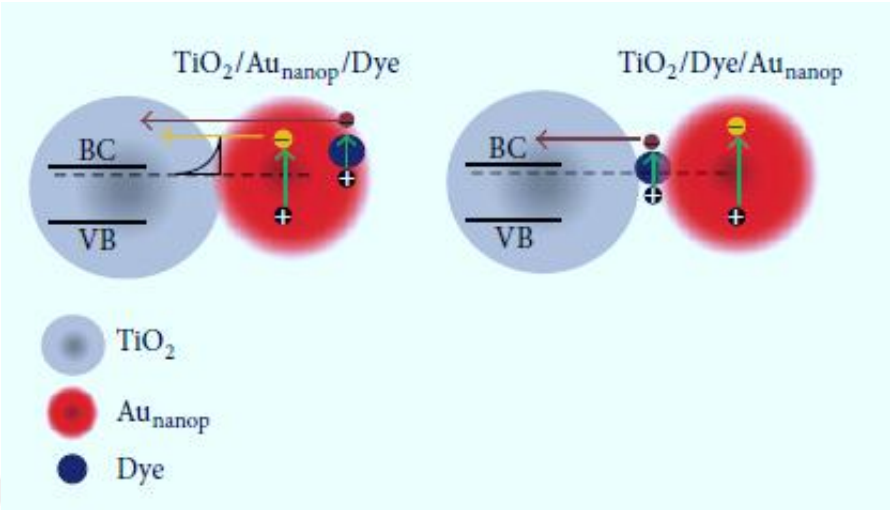

Figure 3.7 Representing the variation of plasmonic excitation for different configuration of devised dye sensitive solar cell [40].

3.5 I-V CHARACTERISTIC OF THE DEVISED ANODIC CONFIGURATION

I-V characteristics of the above mentioned anodic configurations were recorded in potential range of -1 to 1 V under anodic illumination with Pt coated ITO glass as counter electrode. The evaluation was carried by comparing the solar cell characteristics such as such as short-circuit current (Isc), open-circuit voltage (V_{oc}), fill factor (FF), and efficiency (η) for standard cell assembly. The evaluation of plasmonic based DSSC was carried by comparing the obtained characteristics with standard cell assembled without plasmonic nanostructures.

3.5.1 I-V CHARACTERISTIC OF DSSC IN THE ABSENCE OF PLASMONIC NANOSTRUCTURES

The initial study carried with TiO_2 as the anodic base of the solar cell without the usage of plasmonic nanostructures demonstrated relatively small photo-current production as reflected from the corresponding I-V graph shown in the Figure 3.8 I-V plots were recorded both for cell devised with and without compact layer. As seen, the usage of compact layer has proved vital in promoting the overall efficiency and Fill factor of the

solar cell. Thus, usage of compact layer for plasmonic based devised was considered mandatory in the all the experiments. Although, the obtained FF was same the consideration increment in the η of cell devised with compact layer was the consequence of the improvement achieved in the I_{sc} and V_{oc} values. Such increment can be attributed to less loss of photo-current due to re-combination of generated charge carriers at the interfaces associated with mesoporous TiO_2.

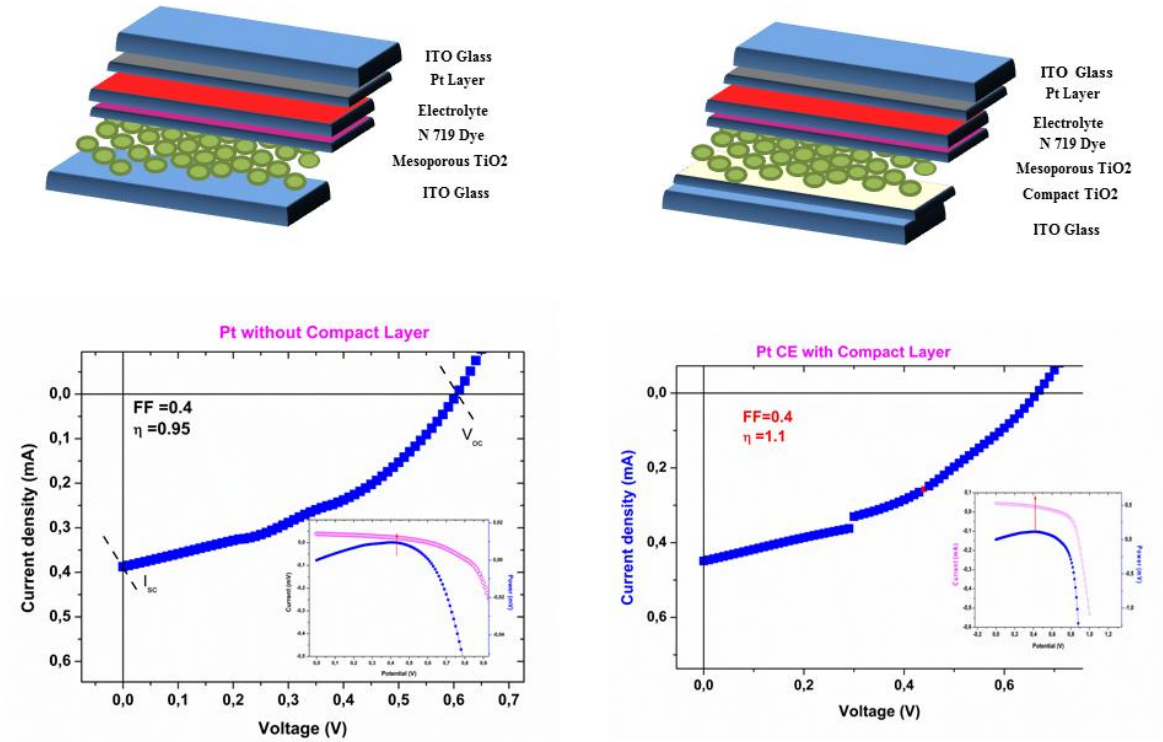

Figure 3.8 I-V characteristics of TiO_2 assisted DSSC in the (a) absence and (b) in the presence of compact scattering layer

3.5.2 I-V CHARACTERISTIC OF DSSC IN THE PRESENCE OF PLASMONIC NANOSTRUCTURES

The plasmonic nanostructures based solar devices were evaluated under similar conditions set for devices assembled without the application of plasmonic nanostructures. The experiment was carried with equal volumes of Ag NCs, Au NSs and Au NCs which were then integrated within the mesoporous anodic layer (TiO_2) to study the variation in the solar cell characteristics as a function of shape and placement of plasmonic nanostructures in DSSC. Since, the placement of plasmonic nanostructures plays as crucial role in the performance enhancement of DSSC, the Au NSs were selected to study the effect of nanostructures placement (mixed within or onto) in the DSSC.

3.5.2.1 I-V CHARACTERISTIC OF AuNS INTEGRATED BOTH MIXED AND ONTO THE MESOPOROUS ANODIC LAYER OF DSSC

The configuration of plasmonic nanostructures can heavily influence the performance of solar device, hence to observe this variation Au NSs were selected for optimization of device configuration. I-V characteristic recorded for Au NSs integrated within and onto mesoporous TiO_2 as shown in Figure 3.9 As seen, the overall improvement in η was observed when Au NSs were integrated within mesoporous TiO_2 attributed to higher I_{sc} value. The FF values were observed not to change in both configuration suggesting the efficiency of Au NSs to act as plasmonic enhancer in DSSC. Based on these experimental results, the intermixing of plasmonic nanostructure within mesoporous layer was considered as the optimum configuration for the devices assembled with Ag NCs and Au NCs.

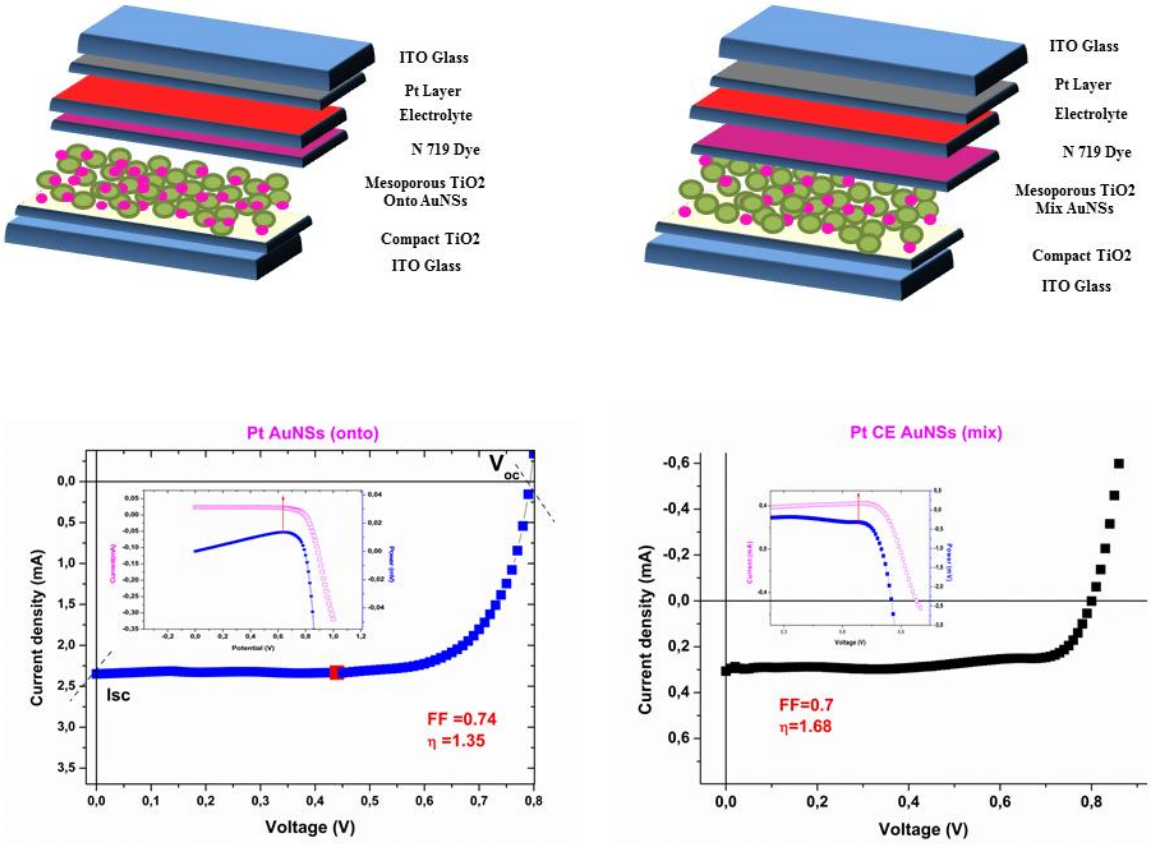

Figure 3.9 Shows the I-V characteristics of Au NSs integrated (a) onto (b) mix mesoporous anodic layer of DSSC

3.5.2.2 I-V PLASMONIC ENHANCEMENT DSSC USING AgNCS AND AuNCS

The plasmonic enhancement associated with Au NCs were elaborately studied against Ag NCs to understand the plasmonic contribution from the cavity containing structures. Figure 3.10 (a) shows the I-V characteristics of Ag NCs integrated within mesoporous layer. As seen, little enhancement has been achieved in this compared to the DSSC prepared without plasmonic nanostructures. However, the usage of Ag NCs have not contributed much to the efficiency in comparison to Au NCs as evident from the I-V curves shown in Figure 3.10 (b). This could be explained on the basic of poor LSPR band overlap with absorption band of N719 dye as seen in Figure 3.1 in section 3.1.1.The insignificant band overlap does not allow significant plasmonic energy transfer to the active energy state of dye which as a consequence decrease the overall absorption capability of sensitizer leading to decline in efficiency. Unlike, Ag NCs the I-V characteristics of Au NCs shows a significant enhancement in the overall efficiency and FF values of devised solar cell. Such significant enhancement may be described as a cumulative effort of various phenomena's occurring simultaneously with the presence of Au NCs. The most of which include, plasmonic energy transfer defined as ''nearfields'', far- field light scattering and hot electron transfer. Although Au NCs LSPR band overlap with N719 dye is relative smaller compared to Au NSs. However, the edge shaped geometry and associated cavity enables much greater plasmonic energy transfer compared to its spherical counterpart[32]. Besides this, the Au NCs have more active area available for dye interaction compared to Ag NCs and Au NSs. The cavity can allow diffusion of dye molecules where enhanced far-field light scattering can easily enable boosting the sensitizing capability of dye. Thus, the greater light scattering, quasi-lighting rod effect associated with Au NCs coupled with plasmonic energy transfer allows Au NCs to boost up the DSSC performance higher compared to Au NSs and Ag NCs. The quasi-light rod effect is most valuable in shapes like cubes and cages. The effect is basically the consequence of the plasmonic energy being concentrated on the edges of the geometry due to metals anisotropic nature. The complete data of Au NCs in comparison to other plasmonic nanostructures have been provided in Table 1.1 As seen, Voc value for plasmonic nanostructure based DSSC is nearly constant. This can be understood as the consequence of fixed temperature. Voc is a function of solar cell temperature. Since during measurement, the solar cells were kept under a fixed

temperature, slight variation was expected with Voc values. An direct and increasing values for Imax can be observed starting from Au NSs. Although, relatively significant improvement has been achieved with the usage of plasmonic nanostructures. The best optimum responses were obtained when Au NCs were taken as the plasmonic nanostructures.

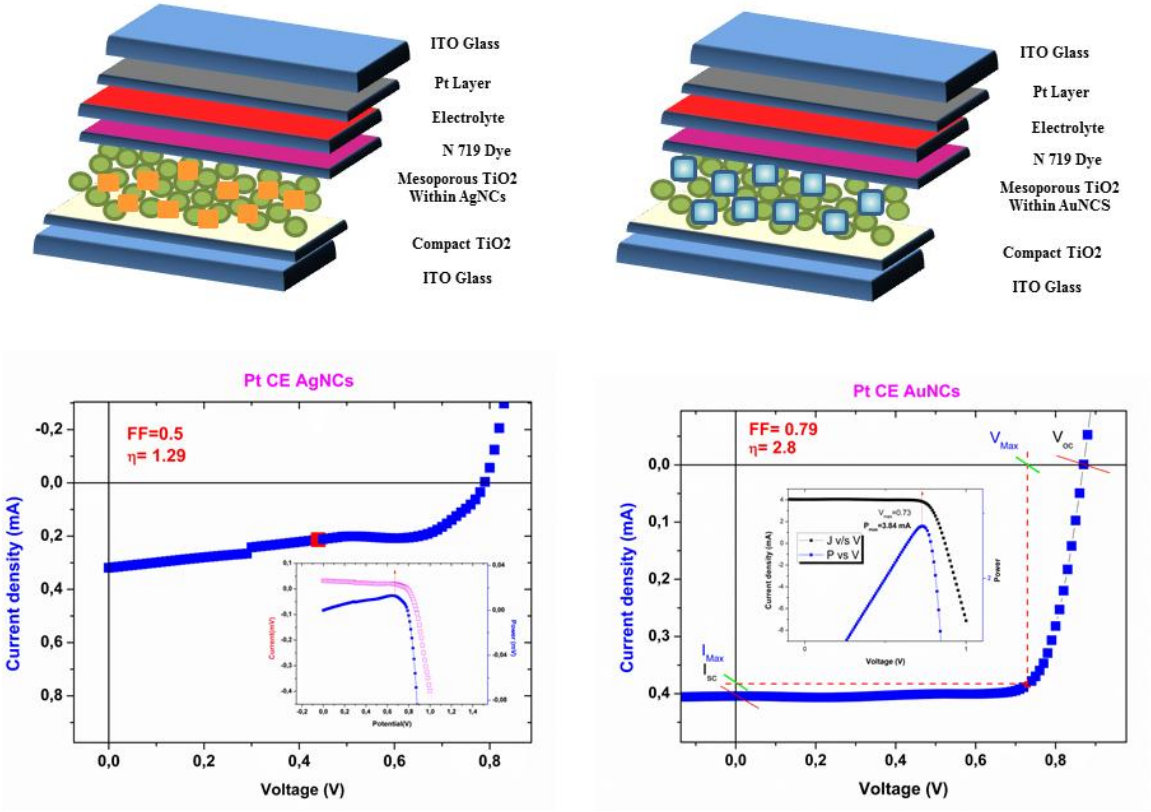

Figure 3.10 I-V curves recorded for (a) Ag NCS and (b) Au NCs integrated in DSSC with inset figure representing power v/s potential graph from P_{max} point

Table 1.1 Shows the overall solar cell characteristics of evaluated from the I-V curves from the plasmonic based DSSC.

Sample	**Isc(mA)**	**Voc (V)**	**Imax(mA)**	**Vmax**	**FF**	**Efficiency**
Pt CE without compact layer and NPs	3.87	0.61	2.31	0.41	0.4	0.95
Pt CE with compact layer	4.5	0.67	2.7	0.41	0.4	1.1
Pt CE Ag NCs(mix)	3.1	0.79	2.03	0.64	0.5	1.29
Pt CE Au NSs(onto)	2.3	0.79	2.12	0.64	0.74	1.35
Pt CE Au NSs(mix)	3.0	0.8	2.4	0.7	0.7	1.68
Pt CE Au NCs(mix)	***4.04***	***0.87***	***3.34***	***0.73***	***0.79***	***2.8***

As seen, the relative increment of 51 and 53% was achieved when Au NCs were used in place of Au NSs and Ag NCs**.**

CHAPTER 4

CONCLUSION

This thesis provides a comprehensive study regarding plasmonic nanostructures based dye sensitized solar cells. The study discusses the synthesis and characterization of various plasmonic nanostructures that can be utilized for the integration within dye sensitized solar cell. The discussed plasmonic nanostructures included silver nanocubes, gold nanospheres and gold nanocages. The as-synthesized nanostructures were elaborately studied for their chemical, compositional and optical characteristics using various analytical techniques such as SEM, TEM and UV-Vis spectroscopy. The as-synthesized nanostructures were then utilized for the integration within the DSSC as the plasmoinc nanostructures. The main aim was to observe the variability of solar cell efficiency with usage of different plasmonic nanostructures. The usage of primarily distinct shaped nanostructures further provided evidences of how the efficiency of solar cell changes with geometry and morphology of the utilized solar cell.

The study, focuses on the plasmonic energy Transfer ability of Au NSs, Ag NCS and Au NCS when embedded within the mesoporous layer of DSSC. Based on the experimental detail Au NCs were found highly promising because of their dual surface area and cage confinement effect. The excellent performance of Au NCs was attributed to the synergetic effect of higher light scattering and lightning rod effect associated with the cavity and the edges of the cage which resulted in the overall amplification in the generation of charge carriers and efficiency of DSSC. The Au NCs integrated in the photo-anodes showed remarkable improvement in PCE value of 2.8% relative to 1.1 % noted for DSSC without plasmonic substrate.

REFERENCES

[1]. Gratzel, M., *Photoelectrochemical cells.* Nature, 2001. **414**(6861): p. 338-344.

[2]. Chapin, F., *Pearson, The Bell Solar Battery.* J. App. Phys, 1954. **25**: p. 676.

[3]. Schiermeier, Q., et al., *Electricity without carbon.* Nature, 2008. **454**(7206): p. 816-823.

[4]. Smil, V., *General energetics: energy in the biosphere and civilization*, in *General energetics: energy in the biosphere and civilization*. 1991, John Wiley & Sons.

[5]. Green, M.A., et al., *Solar cell efficiency tables (Version 45).* Progress in photovoltaics: research and applications, 2015. **23**(1): p. 1-9.

[6]. Hoffmann, W., *PV solar electricity industry: Market growth and perspective.* Solar energy materials and solar cells, 2006. **90**(18): p. 3285-3311.

[7]. Yella, A., et al., *Porphyrin-sensitized solar cells with cobalt (II/III)–based redox electrolyte exceed 12 percent efficiency.* science, 2011. **334**(6056): p. 629-634.

[8]. Hodes, G., *Perovskite-based solar cells.* Science, 2013. **342**(6156): p. 317-318.

[9]. Skotheim, T.A., *Dye-sensitized solar cells*. 1980, Google Patents.

[10]. O'Regan, B. and M. Gratzel, *A low-cost, high-efficiency solar cell based on dye-sensitized colloidal TiO2 films.* Nature, 1991. **353**(6346): p. 737-740.

[11]. Sauvage, F., et al., *Dye-sensitized solar cells employing a single film of mesoporous TiO2 beads achieve power conversion efficiencies over 10%.* Acs Nano, 2010. **4**(8): p. 4420-4425.

[12]. Chapin, D.M., C. Fuller, and G. Pearson, *A new silicon p-n junction photocell for converting solar radiation into electrical power.* Journal of Applied Physics, 1954. **25**(5): p. 676-677.

[13]. Khan, M.I., *A Study on the Optimization of Dye-Sensitized Solar Cells.* 2013.

[14]. Rho, W.-Y., et al., *Recent progress in dye-sensitized solar cells for improving efficiency: TiO 2 nanotube arrays in active layer.* Journal of Nanomaterials, 2015. **2015**: p. 85.

[15]. Fernández, E.F., et al., *Effect of spectral irradiance variations on the performance of highly efficient environment-friendly solar cells.* IEEE Journal of Photovoltaics, 2015. **5**(4): p. 1150-1157.

[16]. Roose, B., S. Pathak, and U. Steiner, *Doping of TiO 2 for sensitized solar cells.* Chemical Society Reviews, 2015. **44**(22): p. 8326-8349.

[17]. Ye, M., et al., *Recent advances in dye-sensitized solar cells: from photoanodes, sensitizers and electrolytes to counter electrodes.* Materials Today, 2015. **18**(3): p. 155-162.

[18]. Baraton, M.-I., *Nano-TiO2 for dye-sensitized solar cells.* Recent patents on nanotechnology, 2012. **6**(1): p. 10-15.

[19]. Martín, C., M. Ziółek, and A. Douhal, *Ultrafast and fast charge separation processes in real dye-sensitized solar cells.* Journal of Photochemistry and Photobiology C: Photochemistry Reviews, 2016. **26**: p. 1-30.

[20]. Boschloo, G. and A. Hagfeldt, *Characteristics of the iodide/triiodide redox mediator in dye-sensitized solar cells.* Accounts of Chemical Research, 2009. **42**(11): p. 1819-1826.

[21]. Wu, J., et al., *Electrolytes in dye-sensitized solar cells.* Chemical Reviews, 2015. **115**(5): p. 2136-2173.

[22]. Zedler, L., et al., *Ruthenium dye functionalized gold nanoparticles and their spectral responses.* RSC Advances, 2012. **2**(10): p. 4463-4471.

[23]. Mahmoud, M. and M. El-Sayed, *Comparative study of the assemblies and the resulting plasmon fields of Langmuir− Blodgett assembled monolayers of silver nanocubes and gold nanocages.* The Journal of Physical Chemistry C, 2008. **112**(37): p. 14618-14625.

[24]. Mahmoud, M.A., B. Snyder, and M.A. El-Sayed, *Surface Plasmon Fields and Coupling in the Hollow Gold Nanoparticles and Surface-Enhanced Raman Spectroscopy. Theory and Experiment.* The Journal of Physical Chemistry C, 2010. **114**(16): p. 7436-7443.

[25]. Mahmoud, M.A., P. Szymanski, and M.A. El-Sayed, *Different methods of increasing the mechanical strength of gold nanocages.* The journal of physical chemistry letters, 2012. **3**(23): p. 3527-3531.

[26]. Myroshnychenko, V., et al., *Modelling the optical response of gold nanoparticles.* Chemical Society Reviews, 2008. **37**(9): p. 1792-1805.

[27]. Sun Y., X.Y., *Shape -controlled synthesis of gold and silver nanoparticles.* Science, 2002. **298(5601)**: p. 2176-2179.

[28]. Rivera, V., E. Marega Jr, and F. Ferri, *Localized surface plasmon resonances: noble metal nanoparticle interaction with rare-earth ions*. 2012: INTECH Open Access Publisher.

[29]. Mahmoud, M. and M. El-Sayed, *Metallic double shell hollow nanocages: the challenges of their synthetic techniques.* Langmuir, 2012. **28**(9): p. 4051-4059.

[30]. Linic, S., P. Christopher, and D.B. Ingram, *Plasmonic-metal nanostructures for efficient conversion of solar to chemical energy.* Nature materials, 2011. **10**(12): p. 911-921.

[31]. Erwin, W.R., et al., *Light trapping in mesoporous solar cells with plasmonic nanostructures.* Energy & Environmental Science, 2016.

[32]. Zarick, H.F., et al., *Enhanced Efficiency in Dye-Sensitized Solar Cells with Shape-Controlled Plasmonic Nanostructures.* ACS Photonics, 2014. **1**(9): p. 806-811.

[33]. Choi, H., et al., *The effect of TiCl 4-treated TiO 2 compact layer on the performance of dye-sensitized solar cell.* Current Applied Physics, 2012. **12**(3): p. 737-741.

[34]. Mbonyiryivuze, A., et al., *Titanium Dioxide Nanoparticles Biosynthesis for Dye Sensitized Solar Cells application: Review.* Physics and Materials Chemistry, 2015. **3**(1): p. 12-17.

[35]. Fillinger, A. and B. Parkinson, *The adsorption behavior of a ruthenium-based sensitizing dye to nanocrystalline TiO2 coverage effects on the external and internal sensitization quantum yields.* Journal of the Electrochemical Society, 1999. **146**(12): p. 4559-4564.

[36]. Lancelle-Beltran, E., et al., *Nanostructured hybrid solar cells based on self-assembled mesoporous titania thin films.* Chemistry of materials, 2006. **18**(26): p. 6152-6156.

[37]. Fang, X., et al., *Effect of the thickness of the Pt film coated on a counter electrode on the performance of a dye-sensitized solar cell.* Journal of Electroanalytical Chemistry, 2004. **570**(2): p. 257-263.

[38]. Jang, Y.H., et al., *Plasmonic dye-sensitized solar cells incorporated with Au-TiO2 nanostructures with tailored configurations.* Nanoscale, 2014. **6**(3): p. 1823-1832.

[39]. Parvez, M.K., et al., *Comparative study of plasma and ion-beam treatment to reduce the oxygen vacancies in TiO 2 and recombination reactions in dye-sensitized solar cells.* Chemical Physics Letters, 2010. **495**(1): p. 69-72.

[40]. Costa de Oliveira, M., et al., *Interface Dependent Plasmon Induced Enhancement in Dye-Sensitized Solar Cells Using Gold Nanoparticles.* Journal of Nanomaterials, 2015. **2015**: p. 9.

[41]. Mahmoud, M.A., D. O'Neil, and M.A. El-Sayed, *Hollow and solid metallic nanoparticles in sensing and in nanocatalysis.* Chemistry of Materials, 2013. **26**(1): p. 44-58.

[42]. Mahmoud, M.A., D. O'Neil, and M.A. El-Sayed, *Hollow and Solid Metallic Nanoparticles in Sensing and in Nanocatalysis.* Chemistry of Materials, 2014. **26**(1): p. 44-58.

[43]. Chen, J., et al., *Facile Synthesis of Gold−Silver Nanocages with Controllable Pores on the Surface.* Journal of the American Chemical Society, 2006. **128**(46): p. 14776-14777.

[44]. *Introduction*, in *Third Generation Photovoltaics: Advanced Solar Energy Conversion*. 2003, Springer Berlin Heidelberg: Berlin, Heidelberg. p. 1-6.

[45]. Haggui, M., et al., *Spatial confinement of electromagnetic hot and cold spots in gold nanocubes.* ACS nano, 2012. **6**(2): p. 1299-1307.

[46]. Rycenga, M., et al., *Generation of Hot Spots with Silver Nanocubes for Single-Molecule Detection by Surface-Enhanced Raman Scattering.* Angewandte Chemie, 2011. **123**(24): p. 5587-5591.

[47]. Rycenga, M., et al., *Surface-enhanced raman scattering: Comparison of three different molecules on single-crystal nanocubes and nanospheres of silver†.* The Journal of Physical Chemistry A, 2009. **113**(16): p. 3932-3939.